INTEGRATION OF AIR POLLUTANT HEALTH IMPACTS INTO ELECTRICITY SYSTEM OPERATION MODELS

A Thesis
Presented to
The Academic Faculty

by

Paul Kerl

In Partial Fulfillment
of the Requirements for the Degree
Doctor of Philosophy in the
H. Milton Stewart School of Industrial and Systems Engineering

Georgia Institute of Technology
December 2016

INTEGRATION OF AIR POLLUTANT HEALTH IMPACTS INTO ELECTRICITY SYSTEM OPERATION MODELS

Approved by:

Professor Valerie Thomas, Advisor
H. Milton Stewart School of Industrial and Systems Engineering
Georgia Institute of Technology

Professor Joel Sokol, Co-Advisor
H. Milton Stewart School of Industrial and Systems Engineering
Georgia Institute of Technology

Professor Ton Dieker
Department of Industrial Engineering and Operations Research
Columbia University

Professor Craig Tovey
H. Milton Stewart School of Industrial and Systems Engineering
Georgia Institute of Technology

Professor Armistead G. Russell
School of Civil and Environmental Engineering
Georgia Institute of Technology

Date Approved: November 10, 2016

To my friends and family.

ACKNOWLEDGEMENTS

First, a thank you to the Strategic Energy Institute at Georgia Tech for supporting a large portion of this thesis, as well as the H. Milton Stewart School of Industrial and Systems Engineering at Georgia Tech for supporting my research and teaching for several years. The encouragement of the Department and those people within continue to push the boundaries of research, and I was lucky to have been able to experience it. I had some idea what to expect coming to Georgia Tech, but those expectations were exceeded in many, many ways.

Second, I would like to thank my advisors, Dr. Valerie Thomas and Dr. Joel Sokol for their endless encouragement, deep questioning, and pushing me to achieve more than I thought was possible. Dr. Thomas and my co-authors had a promising research direction and I am lucky to have been able to be in the right place at the right time and collaborate with such a fantastic group. To Dr. Gary Parker, your advice comes up frequently, and you showed me how great a department one can create with the right puzzle pieces in the right places at the right time. To Dr. Alan Erera, thank you for pushing me towards the end, the positive attitude helped significantly.

Third, thank you to my co-authors, Dr. Wenxian Zhang, Dr. Matthew Realff, Dr. Ted Russell, Dr. Juan Moreno-Cruz and Dr. Athanasios Nenes. Thank you for your continued encouragement and pressure to do better, and to think in new and important ways. Additionally to my committee members, Dr. Craig Tovey, Dr. Ton Dieker, and Dr. Ted Russell, thank you for pushing me in the right direction, and for the memorable advice and teaching.

Fourth, a thank you to my classmates, friends and family. The support has been enormous and has kept me level-headed through my extensive run. Seth Borin in

particular is one of the best friends I could have found, and I would not have met him if not for Georgia Tech ISyE. To Eric Dodge, who has been a helpful and funny friend for over two decades – I appreciate your humor and ideas about high-impact research in air quality. To the many, many others in the ISyE department, thank you for your positive attitudes and friendship.

Finally, a most important thank you to Liz and Kali Collins, your love has helped encourage me to finish, and your positive attitude has helped me immensely. I could not have done it without you and I love you very much.

TABLE OF CONTENTS

LIST OF TABLES

LIST OF FIGURES

SUMMARY

There are extensive impacts on human health due to poor air quality from fossil fuel-based electricity production. The primary aim of this thesis is to integrate air quality models and electricity system optimization models. To minimize both production costs and health impact costs we use a unit commitment electricity generation optimization model fully coupled with an air quality simulation model. A large body of literature exists for air pollutant health impacts, unit commitment optimization models and air quality modeling. However, no work has been previously published that integrates electricity system operation models with temporally resolved pollutant formation and a fine grained spatial resolution of 12km. A major contribution of this research is to integrate these temporally-resolved pollutant formations fully into a unit commitment and dispatch optimization model.

Pollutant exposure depends not only on pollutant source emissions rates. Exposure also depends on the relative location of the power plant to population centers, temperature, wind velocity, cloud cover and sunlight. These atmospheric conditions vary by hour, day, and season. Several models previously were developed that link health impacts to exposure to air pollutants, using non-temporally resolved average values for pollutant formation across time and at the county level. Integrating atmospheric conditions that vary hourly and in three dimensions improves on previous non-temporally dependent pollutant concentration estimates which have under- or over-estimated pollutant concentrations and health impacts.

In Chapter 2, the work presented uses a new finer spatial resolution air quality health impact estimation that varies temporally and can be fully integrated into an

optimization model. The model accounts for atmospheric changes such as wind, temperature, and cloud cover. We developed a method to evaluate fluctuating pollutant formation from source emissions and integrate within an electricity production optimization model. In a case study of the state of Georgia from 2004 to 2011 we show reduced air pollutants and health impacts by shifting production among plants during a select number of hourly periods

In Chapter 3, we define the unit commitment optimization mathematical model and a new objective function which includes both health impact externalities and production costs. We outline the approximations and case study input datasets used throughout the thesis. Finally we illustrate extended results to Chapter 2, including the importance of a higher spatial resolution and the inclusion of a temporal dimension of pollutant formation, which was not included in previous models.

In Chapter 4, we estimate temporally resolved health impacts from three power plants to answer two research questions: 1) if pollutant control technology installation and fuel changes from coal to natural gas were made earlier in July 2007, what would the resulting annual health impacts have been, and 2) what would the heterogeneity in health impacts across racial demographics have been. We apply the method to the State of Georgia for the month of July 2007 vs. July 2015. The research illustrates a new tool to evaluate improvements in health impacts on several demographics. We use a high spatial resolution air quality model that evaluates point sources individually and varies temporally. This model is in contrast to previous modeling which did not use a temporal dimension combined with a higher spatial resolution. These aspects are key when evaluating impacts across demographics and tracking improvements in worst-case hour air quality improvements.

Overall the thesis integrates modeling of pollutant concentration health impacts and electricity generation source emissions. The thesis also provides a strategy for reducing pollutant health impacts using hourly-resolved pollutant concentration formation. Future research can apply these methods more generally and can have a large impact on densely populated areas with high pollutant concentrations.

CHAPTER I

INTRODUCTION

Particulate matter (PM) pollution is a top 10 leading cause of death [23]. Fine particulates less than 2.5 μm in aerodynamic diameter ($PM_{2.5}$) are of particular concern due to higher pollutant concentration exposure causing increases in all-cause mortality, lung cancer mortality and heart disease related mortality, as well as effects on several respiratory-based illnesses including lower respiratory infections; trachea, bronchus, and lung cancers; ischemic heart disease; cerebrovascular disease and chronic obstructive pulmonary disease [23]. These health consequences encourage strategies for the reduction of $PM_{2.5}$ and have important global health benefits. As an example of standards implemented which aim to reduce these air pollutants, the US Environmental Protection Agency (EPA) controls concentrations of $PM_{2.5}$ and O_3 through the National Ambient Air Quality Standards (NAAQS) [41].

Although the NAAQS are important for assessing and creating goals for measured pollutant concentration, to achieve these goals reducing emissions from sources of air pollutants remains a chief concern. In 2013, coal was used to produce 39% of the electricity in the US [34], the largest portion of generation from any fuel type. During combustion, electricity generation from fossil fuels such as coal produce large quantities of primary gaseous pollutants such as sulfur dioxide (SO_2) and nitrogen oxides (NO_X), which are major contributors to air pollution. These gaseous emissions interact with the atmosphere downwind of source emissions, forming several secondary air pollutants including sulfate-based $PM_{2.5}$ and ozone (O_3). Sulfate-based $PM_{2.5}$ composes an estimated average of 24% of the ambient $PM_{2.5}$ in the US [16], and can be controlled in part by a reduction in SO_2 and NO_X emissions. Because of the health impacts of $PM_{2.5}$ and O_3 and acid rain consequences from SO_2 and NO_X emissions, the US EPA has instituted controls and regulations on emissions of SO_2 and NO_X. These have been implemented in part through the acid rain program, which set standards on emissions of SO_2 and NO_X [40].

To assess policy such as NAAQS and the acid rain program, previous air quality modeling has involved extensive multidimensional simulations used to estimate the impacts on pollutant concentrations and health impacts due to changes in emissions [5]. These models account for complex atmospheric conditions and chemistry, including weather conditions such as wind and temperature, and the resultant effects of these factors on pollutant formation [5]. However, these studies generally alter emissions by hypothetically decreasing emissions from all point sources by a fixed percentage, and re-run the multidimensional air quality model. This fixed percentage reduction across all emissions point sources is because the model is a computational burdensome simulation to run for each point source individually [5]. The studies provide an accurate assessment of broad reductions in emissions across multiple point sources. However, the models have limited applicability when needing to run many simulations of different combinations of hypothetical reductions of emissions at point sources [5].

Other studies use a simplified source-receptor framework which approximates how a ton of emissions of SO_2 or NO_X at a point source affects pollutant concentrations of $PM_{2.5}$ and O_3 in downwind counties via Gaussian dispersion air models [25]. These studies ignore the heterogeneous formation of pollutants by hour-of-day (daytime versus nighttime hours) and day-of-year (seasonal changes) that computationally expensive air quality modeling provides [25], but have the advantage of approximating individual point source contributions to pollutant formation downwind [25]. Both types of studies have made major contributions to knowledge regarding air pollutant formation, the effects of reductions in emissions, and the connection of pollutants to emissions sources.

The models outlined above were successfully utilized to recommend new policy measures, and to assess existing policy measures that curb air pollution [25]. These policy measures have included cap-and-trade programs which successfully curbed air pollutant emissions of SO_2 and NO_X, but unfortunately do not handle the spatial and temporal heterogeneity of health impacts due to each ton of emissions having the same valuation within the cap and trade market, regardless of emissions source, time or affected populations downwind [29]. Alternatively, the EPA through NAAQS identifies non-attainment areas, which are defined as areas of the country where air pollution levels persistently exceed NAAQS [41]. These areas are used to regulate nearby emissions sources. Flue gas desulfurization (FGD) reduces SO_2 emissions rates per MWh by up to 97% [45]. Fuel switches from coal to natural gas or other non-emitting generation sources such as solar, hydro, nuclear, wind and certain types of biomass can provide 100% reduction in SO_2 and NO_X emissions [45].

In addition to modeling of pollutants and emission, a separate literature examines the motivation for regulations on the health and environmental impacts of varying levels of pollutant concentrations. These studies utilize measurements of pollutant concentrations from air quality monitoring stations and measured or reported cases of health endpoints such as mortality. They utilize regression methods to measure the causal link between ambient $PM_{2.5}$ concentrations and increased mortality rates or other health conditions and environmental impacts. In particular, mortality rates are connected to pollutant concentration through a concentration-response function (alternatively termed dose-response or exposure-response functions). A small number of these studies are long term and extensive, track broad demographics and numbers of people within the US, their estimated exposure to $PM_{2.5}$, and causes and timing of death. For example, Pope III et al. [28] uses the American Cancer Society Cancer Prevention Study II (ACS CPS-II) and tracks the mortality of approximately 1.2

million adults aged 30 and above. These participants are filtered down to adults which lived near pollutant monitoring stations in metropolitan areas [28], and then examine correlations with concentrations of $PM_{2.5}$ and O_3.

Finally, health benefits equity is an additional goal when implementing new policy. One example evaluation of equity is examining how air quality improvements are distributed across several demographics. Environmental justice is advocated by the US EPA, and is achieved for air pollution, "when everyone enjoys the same degree of protection from environmental and health hazards and equal access to the decision-making process to have a healthy environment in which to live, learn, and work" [47].

1.1 Objectives

In Chapter II, we seek to address the tradeoffs in least-cost electricity production, and the health-based externalities of air pollutants formed downwind of electricity production facilities. The modeling addresses many of the complexities of electricity production and also complexities of health impacts from pollutant concentrations. We seek to answer these questions:

- Is it possible to embed a reduced form version of a multi-dimensional air quality model within an optimization model?
- What are the implications of a temporal dimension of formation within a source-receptor framework at a fine spatial scaling (12 km grid)?
- What are the increased production costs when including monetized health impacts in the objective function?
- At what facilities and fuel types, and at what hours can generation changes occur?

In Chapter 3, we outline the data, assumptions, optimization model, and estimations used within Chapter 2 to derive various case study results. Additionally we explore extended results in the January time horizon vs. July and the sensitivity of the results to the value of a statistical life.

In Chapter 4, we assess the spatial health impacts in greater detail including assessments of demographic and spatial environmental justice concerns. The research seeks to address:

- What are the estimated spatially-resolved health benefits from the policy changes from July 2007 to July 2015?
- Are demographic groups equally benefiting from reductions in emissions?

1.2 Methodology

To address these objectives, in Chapter 2 and 3 we utilize a unit commitment and dispatch optimization model, with linearized estimates of pollutant concentrations due to changes in emissions. The model is run over a retrospective period of 2004 through 2011 during two representative seasonal air quality episodes with hourly temporal resolution covering 31 days in January for winter, and 31 days in July for summer at a 12 km grid resolution. The changes in emissions are assessed between scenarios with two separate but related objectives: minimizing production costs, and minimizing the sum of production costs and monetized health impact costs.

In Chapter 4 we address the spatial capabilities of our model. We analyze the health impacts of July 2015 pollutant control technology installation and fuel changes from coal to natural gas on July 2007 electricity generation. We also analyze the heterogeneity in impacts across race to address environmental justice concerns and find benefits across all demographics examined.

1.3 Contribution

No previous studies have integrated hourly-resolved air emissions impacts on pollutant concentration formation and estimated health impacts within an integrated optimization model. Our contribution is a proof-of-concept demonstration that illustrates the capabilities of an integrated model with a high level of spatial and temporal detail and yields new strategies for controlling pollutant concentrations through fuel use switches among power plants during selected hourly periods. In doing so, we illustrate the importance of a new air quality modeling capability which generates hourly-resolved changes in pollutant concentrations from changes in source emissions.

We also provide an equity assessment of decreases in downwind pollutant concentrations due to reduced emissions. The assessment utilizes the spatial and temporal capabilities of the reductions in emissions by power plant. Our assessment uses high level of detail census tract data including racial and demographic makeup of underlying populations to measure the equitable distribution of health benefits.

CHAPTER II

NEW APPROACH FOR OPTIMAL ELECTRICITY PLANNING AND DISPATCHING WITH HOURLY TIME-SCALE AIR QUALITY AND HEALTH CONSIDERATIONS

Integrating accurate air quality modeling with decision making is hampered by complex atmospheric physics and chemistry and its coupling with atmospheric transport. Existing approaches to accurately model the physics and chemistry lead to significant computational burdens in computing the response of atmospheric concentrations to changes in emissions profiles. By integrating a reduced form of a fully-coupled atmospheric model within a unit commitment optimization model, we allow for the first time a fully dynamical approach towards electricity planning that accurately and rapidly minimizes both cost and health impacts. The reduced form model captures the response of spatially-resolved air pollutant concentrations to changes in electricity generating plant emissions on an hourly basis with accuracy comparable to a comprehensive air quality model. The integrated model allows for the inclusion of human health impacts into cost-based decisions for power plant operation. We use the new capability in a case study of the state of Georgia over the years of 2004 2011, and show that a shift in utilization among existing power plants during selected hourly periods could have provided a health cost savings of \$175.9 million dollars for an additional electricity generation cost of \$83.6 million in 2007 US dollars (USD_{2007}). The case study illustrates how air pollutant health impacts can be cost-effectively minimized by intelligently modulating power plant operations over multi-hour periods, without implementing additional emissions control technologies.

2.1 Introduction

In 2013, coal was used to produce 39% of the electricity in the US [35], the largest portion of generation from any fuel type. During combustion, electricity generation from fossil fuels such as coal produce large quantities of primary gaseous pollutants such as sulfur dioxide (SO_2) and nitrogen oxides (NO_X), which are major contributors to air pollution. These gaseous emissions interact with the atmosphere downwind of source emissions, forming several secondary air pollutants including sulfate-based fine particulates less than 2.5 μm in aerodynamic diameter ($PM_{2.5}$) and ozone (O_3). Sulfate-based $PM_{2.5}$ comprises an estimated average of 24% of the ambient $PM_{2.5}$ in the US [16], and can be controlled in part by a reduction in SO_2 emissions. Increased $PM_{2.5}$ concentrations cause increased mortality and asthma rates as well as non-fatal heart attacks, emergency room (ER) visits, and hospital visits [28]. Previous studies have integrated air pollution impacts into energy system models, but these studies lacked heterogeneous hourly and seasonal temporal pollutant formation. Muller et al. [25],[24] developed the Air Pollution Emission Experiments and Policy analysis model (APEEP) that links air emissions data to monetary and non-monetary damages with county-scale spatial resolution. Siler-Evans et al. [29] evaluated the social benefits of wind and solar power by using EPA emissions data and the APEEP model. They examined changes in damages due to changes in generation within several US sub-regions, using annually averaged impacts from APEEP [29]. Cropper et al. [9] estimated health damages from coal electricity generation in India by combining data on power plant emissions with reduced-form intake fraction models and concentration-response functions for fine particles from [28] to estimate premature cardiopulmonary deaths associated with air emissions. Caiazzo et al. [5] have used the Community Multi-scale Air Quality Model (CMAQ) [4], to assess the health impacts of major emissions sectors in United States. These studies have all made important contributions to the quantitative understanding of the health impacts of air pollution from electricity, transportation, and industrial systems. All, however, use simplified air quality models that assume changes in emissions have homogeneous temporal impacts on pollutant concentration formation (hourly and seasonally), and/or have limited spatial resolution. Due to these simplifications, the models have limited potential for analysis when emissions change at an hourly level.

We introduce the Air Pollutant Optimization Model (APOM) utilizing a new reduced form model capability via the CMAQ decoupled direct method in three dimensions (CMAQ DDM-3D) [49]. The reduced form model provides accurate and fast predictions of air pollutant formation at a sub-county spatial resolution via a 12 km-by-12 km grid, and also provides accurate modeling of heterogeneous temporal formation of air pollutants (Chapter III). Air pollutant emission-concentration sensitivities provided by the CMAQ DDM-3D reduced form model illustrate heterogeneous hourly and seasonal temporal impacts. In addition, because the reduced form model is derived from CMAQ, it provides considerable improvements in linearized estimation of pollutant emission-concentration sensitivities over previous methods [49],[13]. The importance of the linearized model is its computational efficiency and capability for integration with electricity generation commitment and dispatch decision modeling.

In our modeling, we prescribe hourly changes in electricity generation for specific power plants which reduce concentrations of $PM_{2.5}$ downwind of power plants. We use a bottom-up approach, which models individual power plant operation on an hourly level, utilizing a state-of-the-art reduced form atmospheric model directly to predict changes in hourly pollutant concentrations due to changes in emissions from each power plant. We model power plant operations using an electricity generation unit commitment optimization model, with an objective function that includes monetized health impacts. These are estimated via linearized changes in pollutant concentrations from a base case scenario using a \$7.61 million 2007 US dollar (USD_{2007}) value of statistical life (VSL, see Chapter III), and estimated decreases in all-cause mortality rates due to decreases in pollutant concentration from [28]. The first model prescribes optimized operational decisions which minimize production costs, and the second comparison model prescribes decisions with an objective that minimizes both production costs and monetized health impacts. Both of these models are run using identical inputs to provide a comparison between minimizing production costs and minimizing the sum of production costs and monetized health impacts.

Operational decisions from the model which includes monetized health impacts can trade off the increased cost of lower emission alternative-fuel generation, such as natural gas, with the monetized health benefits due to avoided deaths from reduced pollutant concentrations. Primarily these reduced pollutant concentrations are due to lower utilization of coal fueled power plants. Our modeling framework can inform local, state, and national level policy makers of estimates of health consequences on surrounding communities from each power plant, as well as provide actionable ways to reduce pollutant concentrations when pollutant control technology may not be available or installed on SO_2 emitting coal or oil fired plants.

As a case study of our approach, we examine Georgia during two air quality seasons with different electricity generation load patterns [45] and weather scenarios. Specifically we examine the months of July and January, over a retrospective set of years, 2004-2011. The winter air quality season, represented by January 2007, involves electricity-generated heating; the summer air quality season, represented by July 2007, involves extensive use of air conditioning. CMAQ is run for these two months, with reduced form model output then applied to January and July of 2004-2011, adjusting for monthly and yearly differences in electricity demand, population growth, plant emissions rates, fuel costs and plant heat rates.

2.2 Results

We model four of the largest SO_2 emitting electricity generation facilities in Georgia as emissions point sources (shown in Fig.1), and the remaining plants as emissions group sources, grouped by north and south Georgia (shown in Fig.1). Fig.2 shows Plant Bowen as an illustration of health impacts from a representative SO_2-emitting coal plant near a large populated area, for each hour of January 2007 and July 2007 respectively. Fig.2 illustrates the temporal dependence of hourly health costs ($/MWh) from sulfate-based $PM_{2.5}$ formation due to SO_2 emissions. These health impacts reflect heterogeneity in the formation of sulfate-based $PM_{2.5}$ due to SO_2 emissions in summer versus winter seasons in Georgia as well as heterogeneous hour-to-hour $PM_{2.5}$ formation in daytime versus nighttime hours. The seasonal and daytime differences in the formation of $PM_{2.5}$ from SO_2 emissions in Georgia is in part due to increased photochemical activity during summer months and during daylight hours [50]. Fig.2 shows the average impact across the month in green for Plant Bowen, illustrating when health impacts may be under- or over-estimated when not accounting for hourly changes in pollutant formation. While we focus on PM impacts, the method also captures impacts on ozone, but the potential health benefits were found to be dominated by reducing PM. Using a formal sensitivity approach captures the potential for nitrate-replacement, i.e., nitrate increasing when the sulfate is reduced. However, this effect in the southeast (SE) US is rather small, owing to the relative insensitivity of acidity to sulfate reductions for the region [11].

Fig. 3 shows how inclusion of monetized health impacts changes the least cost operation of the electricity generation system in Georgia. In July 2004 natural gas would have been substituted for coal on 20 out of 31 days. With peak generation of approximately 23 GW in July [45], the shifts represent a roughly 25% change in generation on July 5, 2004. Additionally, 12 out of 31 days had a shift in generation greater than 10%. In 2004-2009, the coal plant reductions are primarily from Plant Bowen near

Atlanta, Georgia, the coal fired units at Wansley/Yates and Plant Hammond in north Georgia; the natural gas increases are primarily from the Plant McIntosh Combined Cycle plant near Savannah, Georgia, the gas fired units at Wansley and other natural gas plants throughout the state. Close inspection shows that in 2004 health impact considerations also result in some oil plants displacing coal; the oil is primarily from Plant McManus in Brunswick, Georgia. Decisions during January months are mostly unaffected by health impact costs, in part due to decreased formation of sulfate-based $PM_{2.5}$ from SO_2 emissions from lower photochemical activity in winter months [50]. Additionally, there is lower total and peak electricity demand versus summer months, with a peak generation of approximately 21 GW [45].

Table 1 illustrates \$175.9 million USD_{2007} total avoided health impacts over the

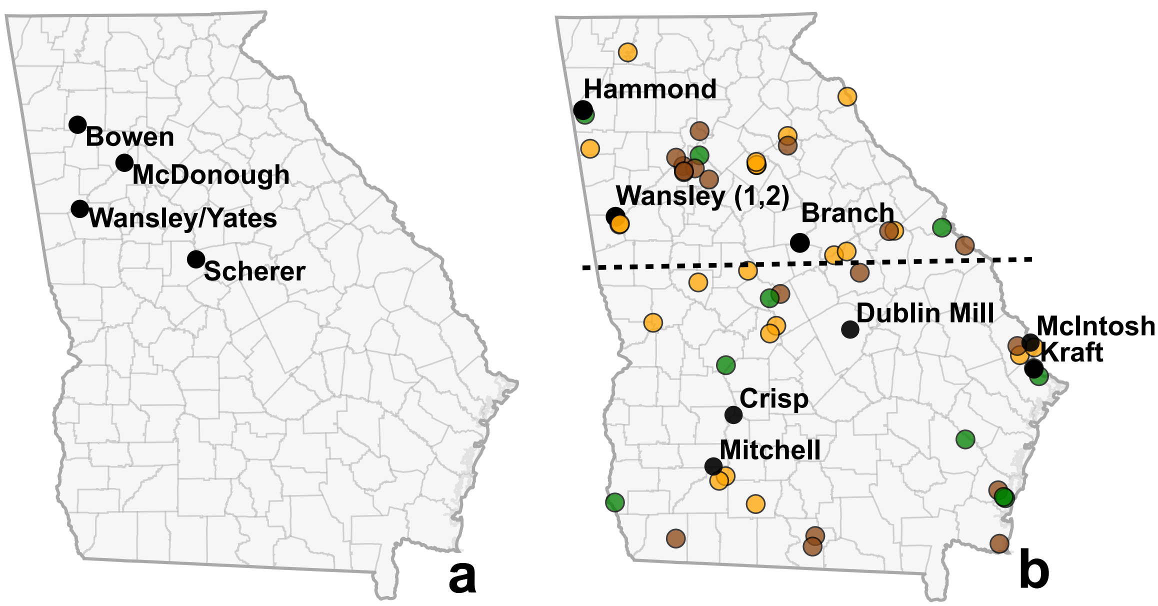

Figure 1: Point and group emissions sources used in the case study, with coal plants shown in black and labeled by name. Fig. 1a represents the location of three point source emitting coal plants and one point source representing a set of coal and natural gas plants (Wansley/Yates). Fig. 1b illustrates the locations of north and south Georgia group source emissions categories, separated by a dashed line (see Chapter III for choice of north and south Georgia split). Biomass plants are green, oil plants are brown, and natural gas plants are orange.

years 2004-2011 for July (see Table 3 for January) with the operating scenario including monetized health impacts versus the operating scenario not including health impacts. The avoided health impacts from 2004-2011 represents a 27.4% decrease of reducible health impacts from the operating scenario which optimizes production costs without health impact costs. The avoided health impacts require a \$83.6 million USD_{2007} increase in production costs for 2004-2011, primarily due to the increased use of more costly natural gas. We also compared the model including temporally resolved pollutant formation with an alternative baseline model which includes average pollutant formation for each plant for the month modeled. The model using

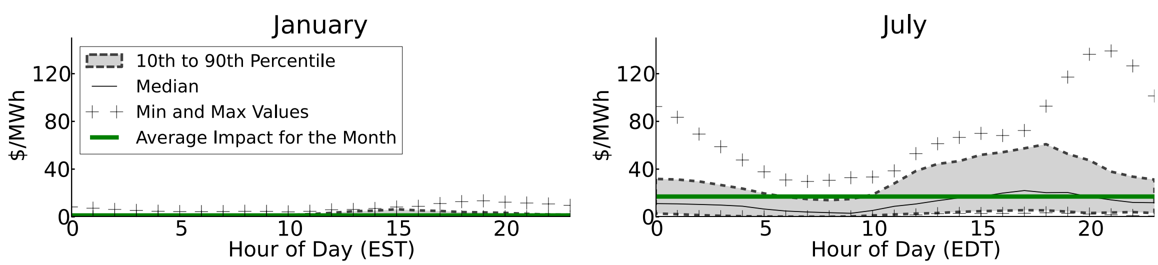

Figure 2: January 2007 (left) and July 2007 (right) median health impacts from secondary $PM_{2.5}$ formation, per unit of generation, by hour of day for Plant Bowen. 10th to 90th percentile values and minimum and maximum values for each day are indicated via the shaded region and plus signs, respectively. The green line indicates the average health impact for the month averaged across all hours in the month. In January Georgia operates on Eastern Standard Time (EST), and in July Georgia operates on Eastern Daylight Time (EDT).

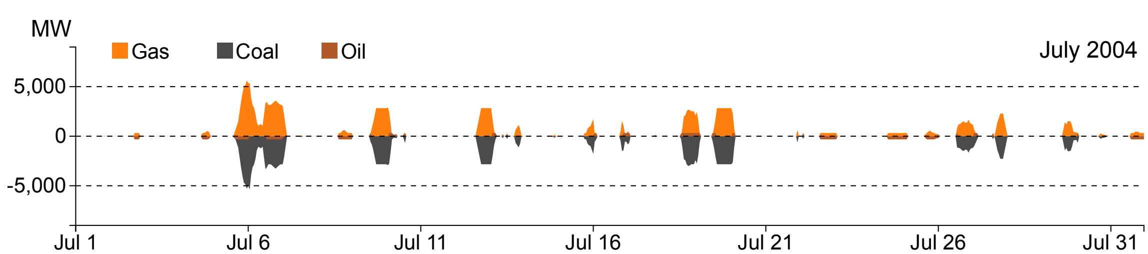

Figure 3: July 2004 hourly difference in fuel use in the scenario minimizing both production cost and monetized health impacts and the scenario minimizing production cost. Positive values indicate more of that fuel being used in the scenario including health impacts. A value of 0 indicates no change during that hourly period between the two scenarios. Note that nuclear, hydro and biomass do not change between the two scenarios, so they are not shown.

Table 1: July monetized difference in health impacts (health costs) in millions USD2007, increased production costs in millions USD2007 and avoided deaths when minimizing the sum of production costs and monetized health impacts, versus minimizing production costs. Percentage of health impact decrease and percentage of production cost increase is given in parentheses.

Year	Health Cost Decrease	Production Cost Increase	Estimated Avoided Deaths
2004	\$25.9 (24.7%)	\$14.01 (4.5%)	3.4
2005	\$11.5 (10.6%)	\$5.58 (1.3%)	1.5
2006	\$36.4 (30.0%)	\$21.10 (4.7%)	4.8
2007	\$39.4 (32.5%)	\$24.93 (5.8%)	5.2
2008	\$24.5 (21.4%)	\$14.21 (3.0%)	3.2
2009	\$5.5 (32.5%)	\$0.56 (0.1%)	0.7
2010	\$23.4 (66.0%)	\$2.10 (0.4%)	3.1
2011	\$9.2 (47.9%)	\$1.08 (0.2%)	1.2
Total	\$175.9 (27.4%)	\$83.57 (2.4%)	23.1

an average pollutant formation and health impact for each plant has health savings of roughly \$62 million USD_{2007}. When including temporally resolved pollutant formation, there is an additional estimated savings of roughly \$114 million USD_{2007} in health impacts. Further, Fig. 2 illustrates the average hourly health impact for Plant Bowen and how temporally resolved health impacts, leveraged within APOM, are heterogeneous when compared to the average impact.

In the later years of our study (2009-2011) some of the largest coal-fired plants in Georgia, Bowen, Wansley, and Hammond, have dramatically decreased SO_2 emissions per MWh due to the installation of flue gas desulfurization (FGD) units. For example, FGD units at Plant Bowen decreased roughly 97% of SO_2 emissions per MWh of generation [45], Chapter III. Fig. 3 shows fuel use changes in July 2004, a representative summer month at the beginning of our time horizon (see Fig. 10 and Fig. 11 for July 2005-2011), and there is similar fuel use change every year during certain days of the month such as July 6th. However, there is less change in fuel use in July 2011 versus July 2004 due to the decrease in emissions rates at several coal plants in 2011 and the lower price of natural gas in 2011 vs. 2004 (see Table 24). Fig. 4 illustrates the unit commitment optimization model average dispatched load for coal and natural gas across each hour of July 2007 for both the scenario including health and the scenario not including health impacts.

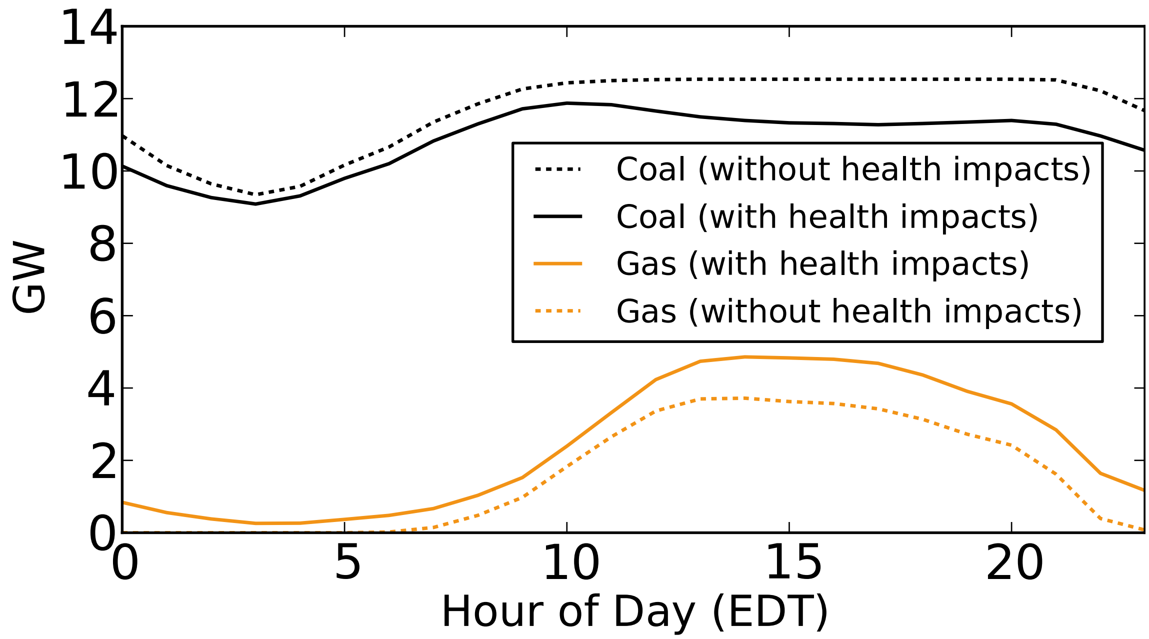

Figure 4: July 2007 average dispatched load by hour-of-day for coal and natural gas plants. The scenario including health impacts is shown by solid lines, and the scenario excluding health impacts is shown by dashed lines.

In addition to aggregated monetized health impacts, we examine each plant in Georgia via disaggregated spatially-resolved changes in health impacts. The two operating scenarios can be compared to each other and to historically observed emissions [45]. As an example of such a comparison, we show spatial impacts for Plant Bowen for the month of July 2007. Plant Bowen, located in northwest Georgia (Fig. 1), is a bituminous coal plant northwest of Atlanta illustrated in Fig. 5 by a red annulus. Plant Bowen had substantial SO_2 pollutant emissions due to large production and due to the use of bituminous, high sulfur coal. The plots shown in Fig. 5 illustrate health impacts from the operating scenario minimizing the cost of production (left), and the scenario minimizing the cost of production and health impacts (right). The right map in Fig. 5 represents a 30% reduction in utilization of Plant Bowen in July 2007. Fig. 5 illustrates differences in monetized health impacts per person for the month of July 2007 from operating the plants to minimize both operating costs and health impacts.

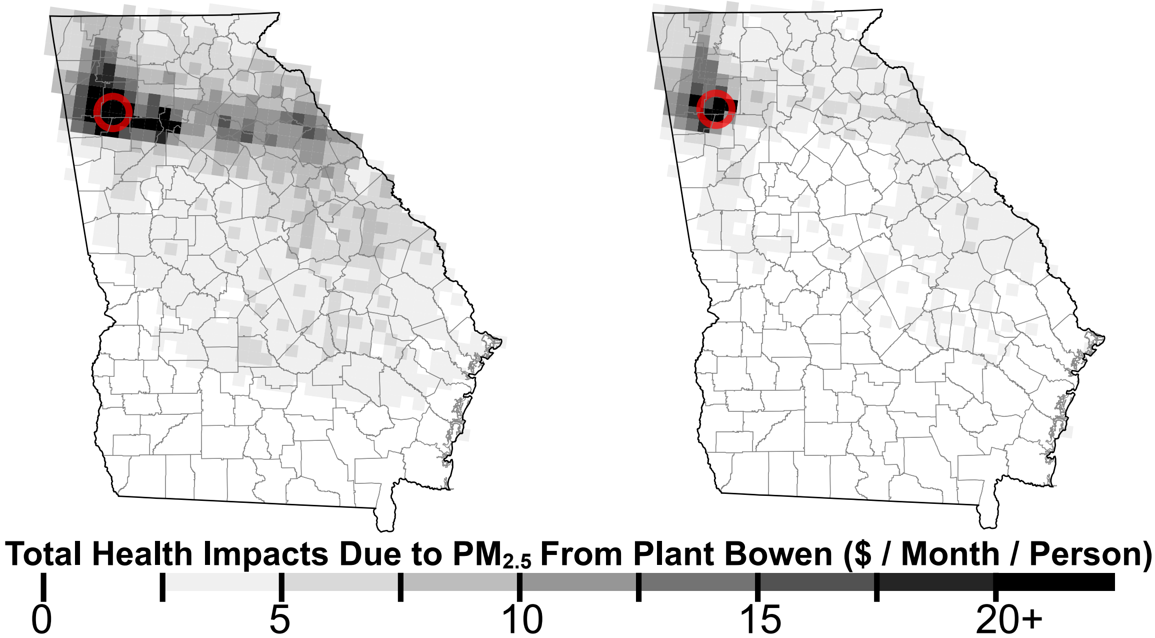

Figure 5: July 2007 total monetized health impact estimates, per person, from Plant Bowen (shown in red), due to secondary formation of $PM_{2.5}$ from SO_2 emissions. The left plot shows health impacts due to emissions health impacts when minimizing production cost, and the right plot shows the health impacts when minimizing both production and health impact cost.

Compared to historically observed emissions, and to the model minimizing production cost, the model which minimizes production costs and monetized health impacts has a large positive effect on health impacts through altered operation of certain power plants such as Plant Bowen. The plot shown in Fig. 6 illustrates the hourly dependence of monetized health impacts for Plant Bowen which averages roughly \$17/MWh of electricity generation in July. \$17/MWh of monetized health impacts at Plant Bowen can be compared to plants in southern Georgia which average less than \$10/MWh in monetized health impacts in July. The difference in health costs is in part due to the transport and transformation of SO_2 into sulfate-based $PM_{2.5}$ near large population areas downwind of Plant Bowen (see Fig. 5). As a reflection of these high health impact costs in July 2007 shown in Fig. 6, the APOM optimization model avoids generation at Plant Bowen during high-health-impact hours or days in years with similar low coal prices relative to natural gas such as 2004-2008 (Table 24), and substitutes with generation at Plant Branch and Kraft (plants with slightly lower emissions rates, further away from populated areas), and natural gas power in locations such as the McIntosh Combined Cycle Facility (south Georgia), the Effingham County Power Plant (south Georgia), the Wansley Combined Cycle Plant (mid-Georgia), and the KGen Murray Combined Cycle Plant (north Georgia) (see Fig. 3 for fuel use changes).

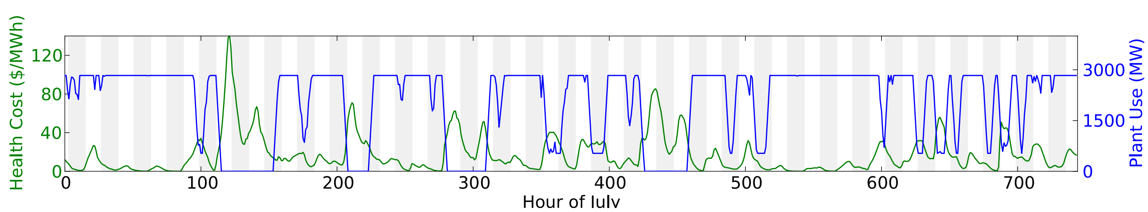

Figure 6: Plant Bowen hourly operation when including health impacts (blue, in MW), and hourly health impacts (green, in $/MWh) for July 2007. Grey areas designate the late evening and morning hours of 11pm to 11am EDT.

APOM decreases Plant Bowen usage by 100% during hours with large health impacts (see Fig. 6), decreasing $PM_{2.5}$ concentrations during several days of July 2007. In the years 2009 and 2011, natural gas generation decreased in cost per MWh relative to coal (see Table 24), reducing the possible health impact savings available through the reduced use of coal. After Bowen fully implemented emission control technology, APOM does not change production levels in 2011 at Plant Bowen due to the significantly lower estimated health impact costs.

2.3 Discussion

Recent developments in air pollutant modeling have created increased capability for policy analysis via more accurate and computationally cheaper reduced form modeling. These reduced form models such as CMAQ DDM-3D provide a necessary solution to the computational burden of running and re-running the full atmospheric model. CMAQ DDM-3D reduced form model sensitivities are generated for each point source for a given emissions scenario a single time, and then can be used and re-used within integrated models, such as the unit commitment optimization model illustrated in our case study. The integration can create innovative air pollutant policy recommendations previously not possible due to the complexity and computational issues involved in modeling a large number of emissions scenarios.

The utilization of CMAQ DDM-3D, as presented here, is what made our new approach possible. The accurate, yet rapid response function of pollutant formation with respect to emissions sources with unprecedented temporal resolution allows for exploration and use of heterogeneous emissions impacts on pollutant formation due to hourly and seasonal differences in weather, wind patterns, and atmospheric chemistry. Operational recommendations differ when taking these hourly impacts into account. Emissions in a given hour versus an earlier hour or later hour may have very different health impacts due to differences in formation and transport of pollutants to populated areas. In particular, nighttime health impacts from emissions versus daytime health impacts from emissions may alter valuation of generation technologies that run more during daytime (solar) or nighttime (wind) hours [29]. In addition, there are seasonal differences that affect air pollutant formation such as the number and intensity of daylight hours [50]. Using an annual or monthly average of monetized health impacts may overvalue or undervalue emissions reductions in peak seasonal periods such as winter and summer, respectively, or miss hourly changes in pollutant formation.

Using APOM for a case study of Georgia over an eight-year period, \$175.8 million USD2007 in monetized avoided mortality are obtainable in the retrospective scenario at a cost of \$83.6 million USD_{2007} in increased production costs. These health impacts gains via decreases in $PM_{2.5}$ concentration are primarily during hours in which formation of $PM_{2.5}$ from SO_2 emissions occurs more readily. Due to the temporally-dependent pollutant formation from SO_2 emissions, we illustrate the groundbreaking use of a temporally-resolved reduced form air pollutant model.

Reduced form model capabilities have increased substantially over the preceding decade [26] and will continue to improve as new research explores ways of estimating pollutant concentration speciation and changes due to emissions more accurately. Research in reduced form models generated online from fully-coupled atmospheric models (such as CMAQ DDM-3D) will advance the modeling framework presented, providing flexible and accurate pollutant formation at an increased resolution in time (sub-hour intervals) and space (sub-12 km grid). Using DDM-3D to forecast source-specific impacts (e.g., EGU and traffic) days in advance is also practical [17], providing operators with needed information in time to plan with existing tools.

While any change in air pollution policy and implementation is challenging, this approach provides the potential to more cost-effectively meet human health and electricity dispatch objectives. Suppose pollution prices are instituted to incorporate temporal and spatial impacts explicitly. Our results suggest that a price schedule that reflects spatial, temporal and seasonal variations increases welfare by not only reducing pollution levels but also by redistributing emissions across space and time. Firms can respond to these types of policies by generating in areas with less potential for high health externalities and shifting their production to periods of time where pollution prices are low. This will require firms to incur costs, but these shifts in location and times have net societal benefits and should be encouraged.

Our new approach can be paradigm shifting, but it will introduce practical challenges associated with the implementation of spatial-temporally resolved policies. First, any such policy needs to adapt to changes in the location and time of polluting activities, as well as secular trends in the economy and technology. This could be addressed by allowing the policy to be reevaluated every five to ten years. Second, the implementation of these policies in the dispatch and operation of the system will require a more efficient decision making process. A price schedule associated with each unit of production that is updated with the same periodicity suggested above is a simple way to incorporate spatially and temporally resolved regulation in the operation of the system. According to our model results, the welfare gains of this policy are substantial and could justify the costs of increased regulation, especially if one considers possible co-benefits to ecosystems and other pollution receptors.

We demonstrate the potential of integrating reduced form air pollutant modeling with a decision model through electricity generation unit commitment and dispatch for the state of Georgia. Our method illustrates how health impacts could be significantly reduced by modulating emissions via power plant operations on a limited, but specific, number of hourly periods. Integrating temporally and spatially detailed air pollutant modeling with operational decision making has not been possible before. Adoption of this approach could identify immediate, cost-effective actions to reduce the health impacts of air emissions from existing energy and industrial systems without additional emissions control technologies. While we have demonstrated its use in Georgia, the approach can be used worldwide.

2.4 Materials and Methods

Our analysis requires several steps. We (i) gather recorded data on historical power plant operation, emissions, and generation load, (ii) run a baseline emissions scenario via CMAQ for two air quality seasons which generates CMAQ DDM-3D reduced form air quality model sensitivities, (iii) link the reduced form air quality model to the unit commitment optimization model via a linearized estimate of monetized health impacts using the reduced form model, (iv) run the minimum cost unit commitment optimization model for the time period and desired months, either including or excluding estimates of monetized air pollutant health impact costs, (v) analyze output from model runs to examine the health impact savings between the model including and excluding monetized health impacts, and (vi) run sensitivity analysis on model inputs to examine how results change due to uncertain input data. Each step is discussed below, and the modeling framework is summarized in Fig. 7.

2.4.1 Data Collection

Electricity generating units (EGUs) characteristics such as fuel type and nameplate capacity are obtained from the EPA Emissions & Generation Resource Integrated Database (eGRID) for the years 2004-2010, with missing years substituted by the most recent past year of data [38]. Capacity factors used for each plant are either fixed for natural gas, coal, biomass, oil and nuclear plants, or set to the annual average value from EPA eGRID for each hydro plant (Chapter III). Hourly generation demand is computed from generation load via hourly load data from EPA Continuous Emissions Monitoring (CEM) and annualized net generation from eGRID (Chapter III), [38]. Fuel costs are from the EIA SEDS database for Georgia and the US [37]. Heat rates are from EIA Electric Power Annual national averages [34], EPA eGRID [38] or EIA AEO 2012 [33] (Chapter III). The Bureau of Labor Statistics Consumer Price Index (CPI) is used to adjust nominal dollar costs to real dollar costs (see Chapter III). Variable operations and maintenance (O&M) costs are from the EIA Electric Power Annual [34], (Chapter III). Fixed O&M costs are from NREL Cost and Performance Assumptions for Modeling Electricity Generation Technologies (see Chapter III).

Plants in Georgia >25 MW in nameplate capacity are required to monitor emissions via the EPA CEM [46]; for plants under 25 MW in capacity, we utilize an emissions rate based on fuel type from EPA eGRID [38]. Fuel for each plant is subtyped into bituminous coal, sub-bituminous coal, residual fuel oil, distillate fuel oil, natural gas, biomass (several subtypes), nuclear and hydro (see Chapter III). Monthly (January or July) average emissions rates are used for coal generation point source plants and Plant Hammond [45], see Chapter III. National annual average SO_2 emissions rates from EPA eGRID are used for fuel subtypes for group source plants [38], (Chapter III).

2.4.2 Emissions Scenario and CMAQ DDM-3D model sensitivities

Within APOM, source emission-concentration sensitivities are used to calculate monetized health impacts. These sensitivities are based on spatially-resolved pollutant concentration estimates simulated by the Community Multiscale Air Quality (CMAQ) model, one of the most widely used chemical transport models in current air quality management [4]. The modeling domain covers the continental US using a 36 km grid resolution with a finer 12 km grid covering the SE US. The meteorological fields are simulated by the Weather Research and Forecasting (WRF) model with four-dimensional data assimilation techniques. The gridded emission rates are prepared by the Sparse Matrix Operator Kernel for Emissions (SMOKE) model using the 2008 National Emissions Inventory (NEI) and 2007 CEM system for nitrogen oxides (NO_X) and sulfur dioxide (SO_2) emissions from EGUs. The model performance is evaluated using the air quality system (AQS) observational data. The performance metrics for 8-hour average ozone and 24-hour average $PM_{2.5}$ concentrations meet US EPA guidelines (see Chapter III) and are summarized in the supporting information (Table 7).

A reduced form model of CMAQ is established using the sensitivities calculated by the embedded direct sensitivity technique, CMAQ DDM-3D [49],[13],[26],[48]. Sensitivities quantify the pollutant-emission response,

$$S_{i,j} = \frac{\partial C_i}{\partial \epsilon_j} \quad (1)$$

where $S_{i,j}$ is the sensitivity of pollutant i to emission rate j; C_i is the concentration of pollutant i; ϵ_j represents the fractional change in emission rate j. Both $S_{i,j}$ and C_i vary with time and location. CMAQ DDM-3D calculates the sensitivities to all the emission rates of interest simultaneously along with simulation of the pollutant concentrations. The reduced form model can be expressed as

$$C_i^* = C_i^0 + \sum_{j=1}^{N} \frac{\partial C_i}{\partial \epsilon_j} \Delta\epsilon_j + \frac{1}{2} \sum_{j=1}^{N} \frac{\partial^2 C_i}{\partial \epsilon_j^2} \Delta\epsilon_j^2 + \sum_{j=1}^{N} \sum_{k=1,k\neq j}^{M} \frac{\partial^2 C_i}{\partial \epsilon_j \partial \epsilon_k} \Delta\epsilon_j \Delta\epsilon_k + H.O.T. \quad (2)$$

where C_i^0 is the baseline concentration of pollutant i; C_i^* is the concentration of pollutant i with perturbation in emission rates of interest; $\Delta\epsilon_j$ is the fractional change in emission rate j and $H.O.T.$ refers to higher order terms. For small changes (up to about 30-50% of total emissions), Cohan et al., [7] have shown that only the first (linear) term is typically required to get an accurate approximation of the response to emission changes thus the second order and higher terms are excluded in our study. The number of sensitivity parameters, N, depends on how many emission sources are of interest. For the case study presented, the sensitivity parameters examined are SO_2 emissions from selected point sources and group sources in Georgia. The resulting reduced form model has been evaluated using the original CMAQ model and has been shown to capture the pollutant-emission response well (Table 7), [49],[13].

2.4.3 Linearized Health Impact Estimate

Monetized health impact costs are estimated via EGU air pollutant emissions rates from point or group sources detailed in the supporting information (Chapter III). Changes in emissions of pollutants such as SO_2 and NO_X cause changes in formation and thus concentrations of O_3 and $PM_{2.5}$ downwind which is modeled using the CMAQ

DDM-3D reduced form model. We use the formation of sulfate $PM_{2.5}$ from SO_2 emissions when calculating and modeling health impacts within the case study, and CMAQ DDM-3D can be used for other species of secondary and primary $PM_{2.5}$ and O_3 [24]. Pollutant concentrations are then connected to health endpoints via linearized approximations of concentration-response functions. Increased $PM_{2.5}$ concentrations have been shown to cause an increase in all-cause mortality [28] and sulfate-based $PM_{2.5}$ comprises the largest portion of reducible health impacts in our study. These sulfate-based $PM_{2.5}$ health impacts are what were used and reported in Table 1. Changes in mortality are then valued via a VSL estimate of \$7.61 million USD_{2007} (see Chapter III for results using alternative VSL estimates).

Spatially-resolved mortality rates and population estimates are used in the health impact valuation step, and match the 12 km geospatial grid resolution (Chapter III). Population varies by year, taken from US Census Bureau population estimates of Georgia (see Chapter III). All-cause mortality estimates are taken from 2010 US Centers for Disease Control and Prevention (CDC) mortality rates by county for Georgia (see Chapter III). Both population and mortality are placed on a 12 km grid, and are taken from the EPA BenMAP database, which uses a population gridding algorithm to estimate population within each 12 km grid square, based on US Census block estimates (see Chapter III).

These calculations provide a linearized estimate of monetized health impacts on a 12 km grid for the state of Georgia on an hourly time scale (see Chapter III for discussion and derivation of linearized estimate). The linearized estimate of monetized health impacts is then used within the unit commitment optimization model of APOM.

2.4.4 Unit Commitment Optimization Model

The optimization component of APOM links an electricity generation unit commitment model with a reduced form air quality model. The optimization model objective is to minimize a summation of both electricity production costs and monetized health impact cost estimates. The electricity production costs include fuel costs, operations and maintenance (O&M) costs, and generation startup costs. The reduced form air quality model adds additional plant-dependent, spatially resolved health impact costs to each unit of power production. These health impact costs are due to $PM_{2.5}$ formed from the emissions of sulfur dioxide. SO_2 forms several species of secondary $PM_{2.5}$, such as inorganic aerosols (sulfate, nitrate and ammonium), and organic aerosols such as organic carbon. We chose to use secondary inorganic sulfate $PM_{2.5}$ formed from SO_2 emissions, which is one of the largest components of secondary $PM_{2.5}$ [16]. Further information on the mathematical formulation used for unit commitment is provided in the Chapter III.

2.4.5 Output Analysis

APOM has several outputs and health cost estimates of interest. The computation of health costs by plant and hour-of-month is generated before running the optimization model. These monetized, population-weighted health impacts present an hourly approximation of emissions impacts on sulfate-based $PM_{2.5}$ pollutant concentrations, and causal chronic health impacts such as increased all-cause mortality. The dispatch strategy output by the optimization model reduces daily and monthly average $PM_{2.5}$ concentrations by reducing $PM_{2.5}$ concentrations during specific prescribed hourly periods. Such a strategy provides specific reductions in hourly periods at EGUs, which is in contrast to a strategy of reducing aggregate SO_2 emissions for a region, or reductions in plant level emissions without specific recommendations as to hour or day these emissions reductions should occur. These hourly estimated health impacts can be further disaggregated spatially, which provides an examination of affected populations, and illustrates where an EGU emissions health impacts are most heavily weighted.

The optimization model outputs prescribed unit commitment and hourly dispatched generation that should occur at each modeled EGU. Load curves can be examined for any inconsistencies with observed historical electricity production, or to describe changes in relative terms to historical operation of plants.

2.4.6 Sensitivity Analysis

Due to the uncertain nature of many of the model parameters sensitivity analysis was run on several sets of input data. One of the most uncertain inputs of the optimization model is the set of hourly emissions-concentration sensitivities. CMAQ model performance is evaluated using air quality system (AQS) observational data, which measures pollutant concentrations hourly at a number of locations throughout the US. The performance metrics for 24-hour average $PM_{2.5}$ concentrations for the modeling domain are summarized in the Table 7, and they are near the acceptable range according to the guidance by [3].

In addition, there are uncertainties in VSL estimation. We examine VSL uncertainty by running a representative month, July 2007, using five VSL estimates which span the range of 26 EPA reported studies (see Chapter III). In addition, there is uncertainty in the estimation of $\beta_{PM_{2.5}}$, which is the causal estimated change in mortality rate due to a change in $PM_{2.5}$ concentration. We use the 95% confidence interval reported by [28] to create a normal distribution for $\beta_{PM_{2.5}}$. We then run the model for 25 random samples from the normal distribution for each of the five VSL estimates to obtain model sensitivity to both $\beta_{PM_{2.5}}$ and VSL simultaneously (see Fig. 13 and Fig. 14).

2.5 Acknowledgments

This work was supported in part by the Georgia Institute of Technology Strategic Energy Institute for the following authors: P. Kerl, W. Zhang, J. Moreno-Cruz, A. Nenes, M. Realff, and V. Thomas.

CHAPTER III

HEALTH IMPACTS DUE TO REDUCTIONS IN ELECTRICITY GENERATION EMISSIONS

3.1 Introduction

Previous models have examined health benefits of displaced emissions, and are discussed in detail in Siler-Evans et al. [29] and summarized here. The first type of model uses average emissions factors that are representative of displacing a fraction of the combined generation from all plants in a region; the second employs regressions of historical data to estimate displaced emissions; and the third approach models the dispatch of generators to explicitly predict the amount of hourly generation and emissions at each generating unit, and can also include detailed grid simulation models to evaluate the impact of displaced emissions [29]. We utilize this third approach, summarized in Fig. 7, integrating a linearized reduced form air quality model which simulates air pollutant concentration impacts within a unit commitment electricity generation optimization model. An integrated approach avoids the computational burden of running a grid simulation model and calculating health impacts for each change in emissions profile.

The supporting information to Chapter II is organized as follows: Section 3.2 discusses the optimization component and mathematical formulation of the unit commitment model, Section 3.3 discuses input data and parameters used, Section 3.4 derives the linear approximation of monetized health impact, Section 3.5 reports extended results and Section A.1 lists tables of model input data used within our model.

3.2 Optimization component

The optimization component of APOM links an electricity generation unit commitment model with a reduced form air quality model. The optimization model objective is to minimize a summation of both electricity production costs and monetized health impact cost estimates. The electricity production costs include fuel costs, operations and maintenance (O&M) costs, and generation startup costs. The reduced form air quality model adds additional plant-dependent, spatially resolved health impact costs to each unit of power production. These health impact costs are due to two secondary air pollutants, ozone (O_3) and fine particulate matter less than 2.5 μm in aerodynamic diameter ($PM_{2.5}$) formed from the emissions of two primary air pollutants, sulfur dioxide (SO_2) and nitrogen oxides (NO_X). SO_2 and NO_X form several species of secondary PM2.5, such as inorganic aerosols (sulfate, nitrate and ammonium), and organic aerosols such as organic carbon. We chose secondary inorganic sulfate $PM_{2.5}$ formed from SO_2 emissions, which is one of the largest components of

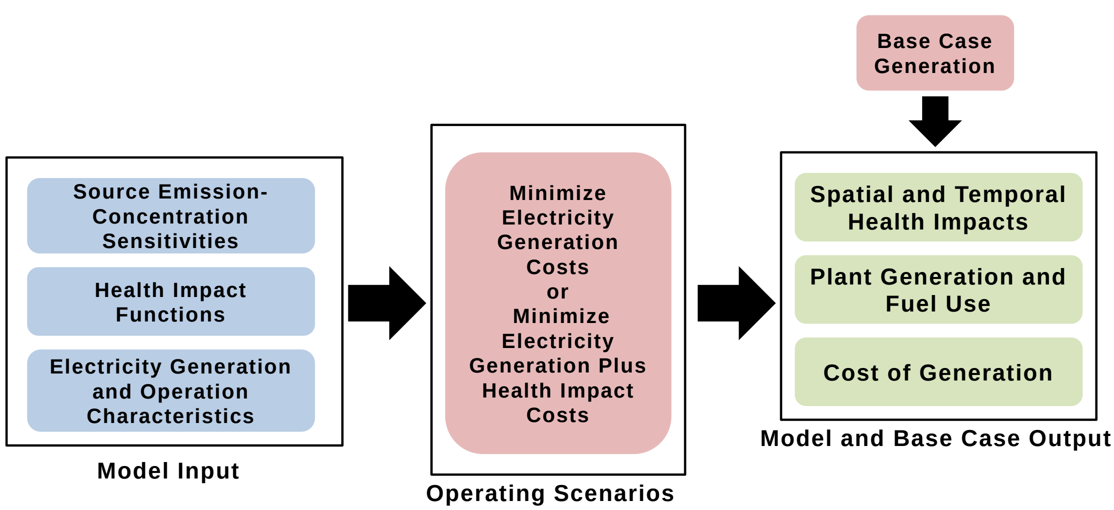

Figure 7: APOM modeling framework including inputs, scenario variants and outputs analyzed.

secondary $PM_{2.5}$. The United States Environmental Protection Agency (EPA) has instituted controls on concentrations of $PM_{2.5}$ and O_3, as well as emissions of SO_2 and NO_X. These have been implemented through the acid rain program and the cross-state air pollution rule, which set standards on emissions of SO_2 and NO_X [40],[44], and the national ambient air quality standards (NAAQS) [41], which set standards for concentrations of $PM_{2.5}$ and O_3.

The optimization model is based on the well-known unit commitment model [15], formulated and solved as a mixed-integer linear programming problem (MILP). The unit commitment model presented here is an electricity production model which coordinates several electricity generators to minimize costs and meet electricity demand. For the case study of Georgia, we formulate the optimization component with Python 2.7 using the gurobipy module, and solve using the Gurobi version 5.1.0 solver [12]. We separate each year and each month, solving each month in a given year as a single unit commitment instance (i.e., July 2007, January 2007, etc...). Because we solve a month-long time horizon versus a shorter time horizon (day or week), we use an optimality gap of 0.25% [1] to ensure that each optimization model run finishes in under roughly four hours of computational time on a 64-bit machine with at least 12GB of memory, with selected runs taking as long as a day of computational time. Sources of cost estimates, power plant characteristics and electricity generation demand inputs for the model are outlined in Section 3.3 and Section A.1.

[1] An optimality gap of 0.25% ensures that the optimized feasible solution is no more than 0.25% more in cost than the true optimal minimum cost. Smaller optimality gaps require longer solve times and more memory. We set the optimality gap using the Gurobi MIPGap parameter.

3.2.1 Mathematical formulation

Several sets and indices are defined that will be used throughout the formulation, summarized as,

I : set of all electricity generating units in Georgia

I_N : set of nuclear fueled electricity generating units in Georgia (note: $I_N \subseteq I$)

G : set of 12 km x 12 km grid squares covering Georgia

H : set of consecutive hours in a given month, the unit commitment time horizon

P : set of primary (source emission) pollutants (SO_2 and NO_X)

Q : set of secondary formed pollutants ($PM_{2.5}$ and O_3).

Each set will be indexed by the lowercase letter of the set. For example, index i refers to an electricity generating unit in I.

3.2.1.1 Cost estimates

Several cost estimates are used in the linearized objective function. These cost estimates have been discounted to year 2007 US dollars using the CPI values in Table 23,

F_i = fuel cost of plant i (\$ / MWh)

R_i = variable operations and maintenance cost of plant i (\$ / hour committed)

T_i = startup cost of plant i (\$ / startup)

$A_{i,h}$ = air quality health impact costs at plant i, hour h (\$ / MWh).

3.2.1.2 Parameters

Several input parameters are used either to construct a cost estimate, or within the constraints of the model. The parameters below indicate electricity demand, specific plant characteristics, health impact parameters, and pollutant concentration emission sensitivities from the reduced form model,

d_h = electricity demand in hour h (MWh)

δ_i = maximum instantaneous capacity factor of plant i, as a percentage of plant i's capacity

N_i = nameplate capacity of plant i (MW)

β^q = percent increase in all-cause mortality due to an increase in concentration of secondary pollutant q

VSL = value of a statistical life ($ per life lost in USD2007)

$e^p_{i,h}$ = emissions rate of primary pollutant p from plant i, in hour h (lbs / MWh)

$E^p_{i,h}$ = baseline total emissions of primary pollutant p from plant i, in hour h (lbs)

M_g = hourly mortality rate in grid square g

POP_g =population in grid square g

$S^{p,q}_{i,h,g}$ = increase in concentration of secondary pollutant q, in grid square g, due to the percent change in baseline emissions of primary pollutant p from plant i, in hour h

τ^i = if committed, the minimum amount of generation required at plant i (as a percentage of plant capacity)

μ^i = the maximum ramp rate up/down at plant i as a percentage of plant i's capacity.

3.2.1.3 Decision variables

Four sets of decision variables are used for the unit commitment model. The decision variables represent optimized decisions that indicate if a generator is committed for that hour (binary variable, 1 or 0), if a plant should be started in a given hour (binary variable, 1 or 0), if a plant should be shut down in a given hour (binary variable, 1 or 0), and finally, if committed, the amount of electricity that should be generated in that hour (a continuous variable),

$z_{i,h}$ = electricity generated by plant i, in hour h (MWh)

$u_{i,h}$ = binary unit commitment variable for plant i, in hour h (0 down, 1 operational)

$v_{i,h}$ = binary startup variable for plant i, in hour h (1 for startup, 0 otherwise)

$w_{i,h}$ = binary shutdown variable for plant i, in hour h (1 for shutdown, 0 otherwise).

3.2.1.4 Air quality health impact cost ($ / MWh)

Using the previously defined parameters, health cost estimates in units of \$/MWh are calculated using population data, mortality rates, value of a statistical life (VSL), emissions rates of primary pollutants SO_2 and NO_X, and the concentration-response function estimates for O_3 and $PM_{2.5}$. Note that for the case study of Georgia, we used sulfate-based $PM_{2.5}$ formed from SO_2 emissions, but the formulation shown is more general. For notational convenience, it is helpful to define these air quality health impact cost estimates separately before they appear in the objective function,

$$A_{i,h} = VSL \sum_{p \in P} \sum_{q \in Q} \beta^q (e^p_{i,h})/(E^p_{i,h}) \sum_{g \in G} M_g POP_g S^{p,q}_{i,h,g}.$$

3.2.1.5 Objective function

The objective function is defined as,

$$min \sum_{h \in H} \sum_{i \in I} \left[(F_i + A_{i,h}) z_{i,h} + R_i u_{i,h} + T_i v_{i,h} \right],$$

with the sum across all hours of the given time horizon, and across all generating plants. These costs include fuel costs (F_i), additional optional air quality health impact costs ($A_{i,h}$), variable operations and maintenance costs if a plant is committed

(R_i), and startup costs when a plant is first committed (T_i). Note that when minimizing only production costs, the air quality health impact costs $A_{i,h}$ are removed from the objective function.

3.2.1.6 Unit commitment constraints

Generation unit commitment is a well-known difficult problem [14], and can be formulated in several equivalent ways [14] as a mixed integer linear program (MILP). We use the strongest formulation outlined in [14], which defines logical constraints for the startup, shutdown and unit commitment binary variables in ways that are facet defining. Facet-defining valid inequalities generally produce faster computational running times [27]. These constraints are defined in detail below, which are equivalent to equations [1], [7] and [8] in [14], respectively,

$v_{i,h} - w_{i,h} = u_{i,h} - u_{i,h-1},\ \forall i, h \in H \backslash \{0\}$, equation defining the logical relationship between startup, shutdown and on/off binary variables

$v_{i,h} \leq u_{i,h},\ \forall i \in I, h \in H$, inequality requiring a unit that is turned on to be operating at that time

$w_{i,h} \leq 1 - u_{i,h},\ \forall i \in I, h \in H$, inequality requiring that a unit turned off at time h cannot be operating at that time.

3.2.1.7 Ramping constraints

In addition to unit commitment constraints, we impose constraints on the ramp-up and ramp-down in generation from one hour to the next. Here we limit ramp-up and ramp-down to $\mu^i = 25\%$ per hour for coal plants. Further analysis of the choice of ramp rate is given in Section 3.3. Ramp rates are unrestricted for natural gas plants and hydro power plants (equivalent to possible ramping of $\mu^i = 100\%$ of capacity within an hour). For nuclear plants, there is an additional minimum required amount of generation, so generation is restricted within the range of 80% (minimum generation allowed for nuclear plants) and 95% (capacity factor for nuclear) of nameplate capacity. Note that due to this minimum required generation for nuclear, nuclear plants are assumed to be committed in all hours. Recall that ϕ_i is the maximum instantaneous capacity factor of plant i (as a percentage of capacity), and N_i is the nameplate capacity of plant i (in MW). Also note that in the 0th hour of the month we assume that a plant can start at any feasible generation level to account for the cutoff in our model before the 0th hour.

$$
\begin{aligned}
z_{i,h} - z_{i,h-1} &\leq \phi_i N_i \mu^i, \ \forall i \in I, h \in H \backslash \{0\}, \text{ maximum ramp-up constraint} \\
z_{i,h-1} - z_{i,h} &\leq \phi_i N_i \mu^i, \ \forall i \in I, h \in H \backslash \{0\}, \text{ maximum ramp-down constraint} \\
z_{i,h} &\geq N_i \tau^i \ \forall i \in I_N, h \in H, \text{ minimum generation constraint for nuclear plants}
\end{aligned}
$$

3.2.1.8 Generation constraints

We also are required to meet electricity demand using committed plant generation in each hour. Furthermore, each plant can generate no more than its available capacity, and if committed, certain base load plants, such as nuclear and coal, must comply with minimum capacity requirements.

$$
\begin{aligned}
z_{i,h} &\leq \phi_i N_i u_{i,h}, \forall i \in I, h \in H, \text{ maximum generation constraint, if committed} \\
z_{i,h} &\geq \tau^i \phi_i N_i u_{i,h}, \forall i \in I, h \in H, \text{ minimum generation constraint, if committed} \\
\sum_{i \in I} z_{i,h} &= d_h, \forall h \in H, \text{ electricity demand must be satisfied.}
\end{aligned}
$$

3.2.1.9 Binary and non-negativity restrictions

Finally, the unit commitment variables are restricted to be binary (0 or 1), and other variables such as generation must be non-negative,

$$z_{i,h} \geq 0, \forall i \in I, h \in H, \text{ generation variables are non-negative}$$

$$u_{i,h} \in \{0,1\}, \forall i \in I, h \in H, \text{ unit commitment variables are 0 or 1}$$

$$v_{i,h} \in \{0,1\}, \forall i \in I, h \in H, \text{ start-up variables are 0 or 1}$$

$$w_{i,h} \in \{0,1\}, \forall i \in I, h \in H, \text{ shut-down variables are 0 or 1.}$$

3.3 Input data and parameters

3.3.0.10 Electricity generation load

For this study, we assume that generation of all plants within the state lines of Georgia listed by the EPA eGRID database can be controlled, including large plants partially owned by Georgia Power and other non-Georgia Power generating facilities operating within the state.

Electricity demand is estimated by aggregating the load of all plants within the state of Georgia. We first sum generation load values for each hour (0 to 23) of each day (1 to 31) in each month (January and July) of each year, 2004-2011. The first summed value uses EPA Continuous Emissions Monitoring (CEM) hourly loads (megawatt load multiplied by percent of each hour the plant was operated) aggregated across all emitting power plants in Georgia, for each hour of each day [45]. Because EPA CEM data does not include zero emissions plants such as nuclear and hydro, we need to add an estimated amount for those plants. The estimated amount uses annualized net generation from nuclear and hydro power plants in the EPA eGRID 2009 dataset [38], which is then divided by 365 days, and then 24 hours to provide an estimated average hourly generation from nuclear and hydro.

3.3.0.11 Power plant characteristics

Power plant characteristics such as nameplate capacity, annual capacity factors (the ratio of average hourly net generation in MW to name plate capacity in MW), latitude and longitude, plant prime mover (steam generator, gas turbine, internal combustion or combined cycle) and fuel type (natural gas, coal type, etc.) of a plant are taken from the EPA eGRID 2009 dataset [38], and shown in Tables 34, 35, 36 and, 37 in Section A.1.

Maximum capacity factors are increased for coal and natural gas to 80% of nameplate capacity, due to EPA eGRID values reporting an average capacity factor versus a maximum capacity factor. Emissions rates of SO_2 and NO_X from EPA CEM hourly measurements of EGUs are used to establish plant baseline emissions for January 2007 and July 2007 and also to measure average emissions rates for point source emissions plants and for Plant Hammond [45]. For group source plants other than Plant Hammond, for each year we estimate an emissions rate based on fuel type, either via the US annual average for the fuel type or via the Georgia state annual average for that fuel type as reported in EPA eGRID in the most recent measured year [38]. Fuel for each plant is sub-typed into bituminous coal, sub-bituminous coal, residual fuel oil, distillate fuel oil, natural gas, biomass (several subtypes), nuclear and hydro (see Table 29, Table 30, Table 31 and Table 32 for emissions rates used).

3.3.0.12 Power plant ramping constraints

Coal power plants and natural gas plants cannot be switched to full power or down from full power instantaneously. In this model, we use ramp-up and ramp-down rates of four hours to and from full capacity for coal plants (25% per hour), which accounts for starting several boilers at larger plants such as Plant Bowen (e.g., four separate boilers for Bowen). We assume no restriction on ramping for natural gas plants, oil plants, hydro plants or nuclear plants. For nuclear, however, we assume a minimum generation of 80% of name plate capacity to model nuclear as always-on base load generation. In the literature, [1] use a full-capacity ramp-up and ramp-down time of three hours for coal (33% per hour) and two hours for natural gas (50% per hour). [20] analyze generator response to intra-hour load fluctuations and note that coal units can respond at 1% to 3% of their current load per minute, and combustion turbines at 10% to 20% of current load per minute. Load changes at Plant Bowen and Plant Scherer (including all boilers) are examined across the hours of July 2007 using EPA CEM data [45]. The maximum observed ramp rate up for Plant Bowen was 690 MW per hour (19.7% of nameplate capacity) and 701 MW (19.9% of nameplate capacity) for Scherer, while maximum ramp rates down were 530 MW (15.1%) for Bowen and 736 MW (20.9%) for Scherer.

Based on the literature and observed behavior of plants Bowen and Scherer, for coal fired plants we use a maximum ramp rate up and down of 25%. However, to account for different ramping conditions, we then also ran the unit commitment model with maximum ramp rates up and down of 150 MW per hour to 400 MW per hour in 50 MW increments, and separately ramp rate percentages of 15% to 50% of nameplate capacity (adjusting minimum load requirement constraints when using lower ramp rate values). These did not substantially alter results (no more than 10% change in health impacts), but do alter power plant generating load patterns.

3.3.0.13 Plant fuel costs and operations and maintenance costs

Plant fuel costs and variable operation and maintenance (O&M) costs are estimated for the following fuel type and sub-types: hydro, natural gas, coal (sub-bituminous and bituminous), nuclear (U3O8), petroleum (residual fuel oil, distillate fuel oil and petroleum coke) and biomass (wood and waste, landfill gas, municipal solid waste and black liquor). Fuel costs are estimated by year for the state of Georgia, when possible, using historical data from the EIA State Energy Data System (EIA SEDS) database [37]. Further detail on startup cost by fuel type, fuel cost, variable O&M and fixed O&M source data is available in Section A.1.

3.3.0.14 Population

2010 US Census population block-level data were used to create a geographical profile of population across the state of Georgia using the air quality simulations 12-km-by-12 km grid via the US EPA BenMap tool [43]. Populations for 2004-2009 and 2011 are made using intercensal estimates shown in Table 38. A census block is the smallest geographical unit used by the US Census Bureau for tabulation of data collected on population. Blocks are defined by natural boundaries such as streets, roads, railroads, streams or other bodies of water, or other natural boundaries [32]. There were 291,086 census blocks used for Georgia in the 2010 US Census, and roughly 1,100 12 km-by-12 km grid-squares used to geographically represent Georgia in the CMAQ air quality model. The US Census 2010 block level population data aggregated into 12 km-by-12 km grid cells was taken from the EPA BenMAP software tool [43] and shown in Fig. 8.

3.3.0.15 Mortality rates

All-cause mortality data are from the year 2010 US Centers for Disease Control and Prevention mortality rates by county for Georgia [6]. These mortality rates were used in calculating the change in mortality due to changes in pollutant concentrations within a 12 km grid cell [43]. These mortality rate estimates were taken from aggregated 12 km grid cells via the EPA BenMAP software tool [43]. All-cause mortality rates for ages 30-99 are shown in Fig. 8.

3.3.0.16 Health impact estimates

This study uses estimates of a change in mortality rate due to a change in $PM_{2.5}$ concentration. Estimates typically utilize outdoor measured pollutant concentration as a proxy for pollutant exposure within a population. We use the results of a study from [28] to approximate the effects of $PM_{2.5}$ pollutant concentration on all-cause mortality, sometimes termed exposure-response, but also dose-response or concentration-response. Table 2 lists the relative risk (RR) ratio utilized in this study.

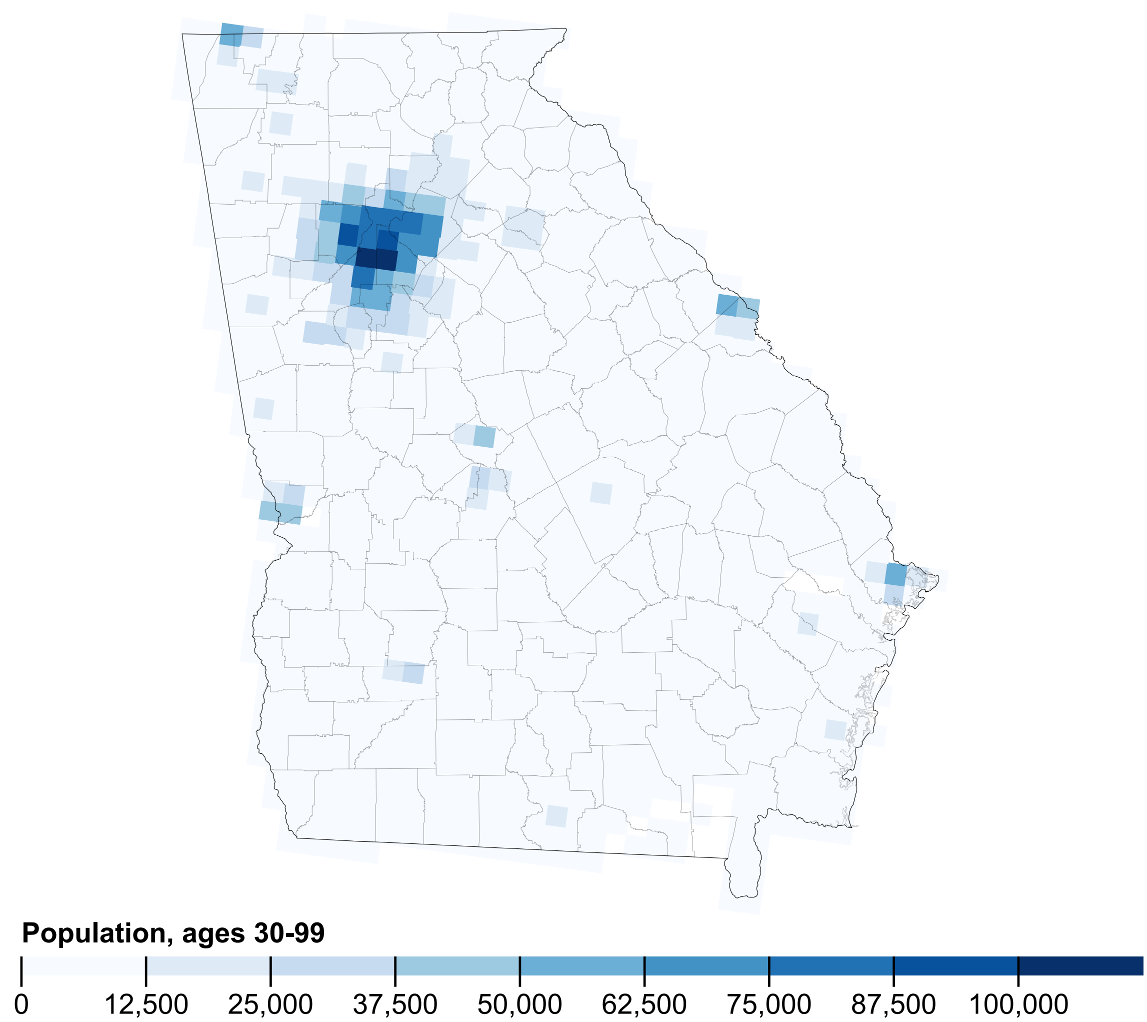

Figure 8: Georgia 2010 US Census population, ages 30 to 99

Table 2: Adjusted all-cause mortality relative risk (RR) ratio associated with a 10 μg/m^3 increase in $PM_{2.5}$ concentration. 95% confidence interval is shown in parentheses.

	All-cause mortality
Pope (2002)	1.06 (1.02-1.11)

3.3.0.17 *Value of a statistical life estimate*

The value of a statistical life (VSL) is a method to assess the economic value of eliminating the risk of one premature death [39]. By using VSL, comparing the monetized effects of changes in concentration with changes in the costs of production

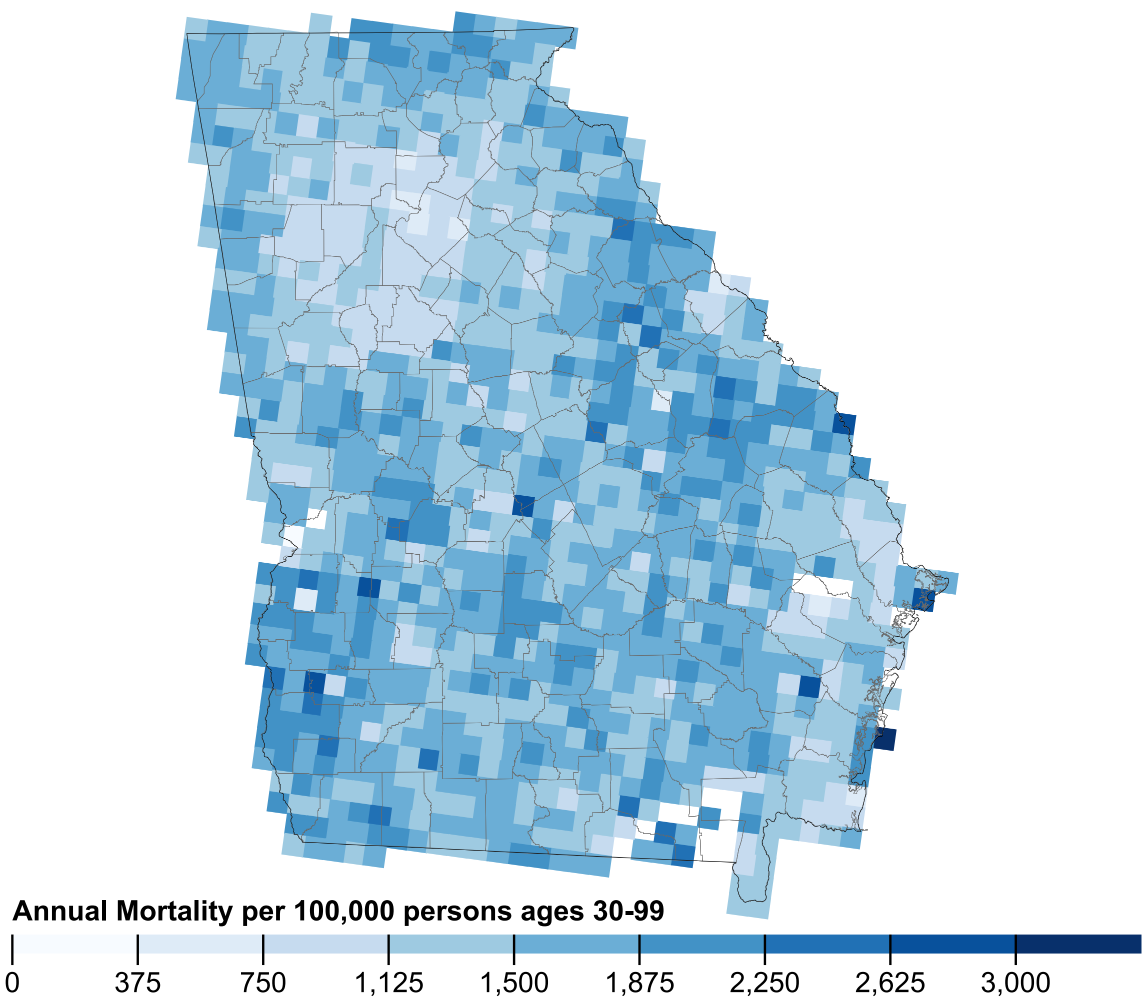

Figure 9: Georgia annual mortality rate per 100,000 persons, ages 30 to 99

is possible within an integrated model. Guidance is taken from the US EPA Guidelines for Preparing Economic Analyses: Mortality Risk Valuation Estimates [39]. For this study we use the median value of $7.61 million (adjusted to USD_{2007} using US GDP deflators) advised by the EPA [39]. The 26 VSL estimates used are shown in Section A.1. [21] explores VSL revealed preferences and stated preferences in detail.

3.4 Health concentration response functions and linearization

In previous studies health endpoints such as mortality have been connected to air pollutant concentrations of $PM_{2.5}$ through a concentration-response (CR) function [28],[22]. These functions are log-linear, and provide a method of predicting how a change in air pollutant concentration will change the observed incidence of a health endpoint such as mortality for a specified region. This systematic process can be implemented for a gridded region over a specified time horizon using specialized tools such as BenMAP from the US EPA [43]. Alternatively, one can use the CR functions that are utilized within BenMAP [43] or are reported in the literature [28] to quantify the effects of each air pollutant over a specified location (i.e., grid square). We use this second method within the mixed-integer linear programming (MILP) formulation, with a linearized approximation of a log-linear relationship between a change in pollutant concentration and a change in mortality.

The shape of CR functions varies depending on the epidemiological study and pollutant examined, such as $PM_{2.5}$ or O_3. For $PM_{2.5}$, log-linear CR functions have been recommended; alternatives include threshold functions or splines [28],[10]. In this study, we use a linearized approximation of a log-linear relationship between pollutant concentration and mortality, which takes the form below. The model follows from a regression model used by [28] and uses the following notation,

$$
\begin{aligned}
y_{d,t} &= \text{observed mortality on day d, year t} \\
Y_{d,t} &= \text{random variable representing mortality on day d, year t} \\
u_{d,t} &= E[Y_{d,t}] = \text{ expected mortality rate on day d, year t} \\
u^*_{d,t} &= E[Y^*_{d,t}] = \text{ perturbed expected mortality rate on day d, year t} \\
\Delta u_{d,t} &= u_{d,t} - u^*_{d,t} = \text{ change in expected mortality rate on day d, year t} \\
\beta_{PM_{2.5}} &= \text{log-relative rate of increase} \\
&\quad \text{in mortality associated with an increase in PM}_{2.5}\text{ concentration} \\
C^0_{d,t,PM_{2.5}} &= \text{baseline mean concentration of PM}_{2.5}\text{ on day d, year t} \\
C^*_{d,t,PM_{2.5}} &= \text{perturbed mean concentration of PM}_{2.5}\text{ on day d, year t} \\
\Delta C_{d,t,PM_{2.5}} &= C^*_{d,t,PM_{2.5}} - C^0_{d,t,PM_{2.5}} = \text{ the change in concentration of PM}_{2.5} \\
&\qquad \text{on day d, year t}
\end{aligned}
$$

The expected mortality rate can be modeled as a log-linear regression model such as the Cox proportional hazards model:

$$\log u_{d,t} = \beta_{PM_{2.5}} C^0_{d,t,PM_{2.5}} + \alpha.$$

α represents remaining confounding factors and variables used as controls for mortality by the specific study, following the notation followed by the EPA BenMAP manual [42]. For example, [28] control for factors such as random spatial effects, age, sex, race, smoking, education level, diet, etc. Next we take the difference in log-expected mortality rate on day d and our perturbed estimate.

$$
\begin{aligned}
log(u^*_{d,t}) &= \beta_{PM_{2.5}} C^*_{d,t,PM_{2.5}} + \alpha \\
&= \beta_{PM_{2.5}} C^*_{d,t,PM_{2.5}} + \alpha + \beta_{PM_{2.5}} C^0_{d,t,PM_{2.5}} - \beta_{PM_{2.5}} C^0_{d,t,PM_{2.5}} \\
&= \beta_{PM_{2.5}} C^0_{d,t,PM_{2.5}} + \alpha + \beta_{PM_{2.5}} (C^*_{d,t,PM_{2.5}} - C^0_{d,t,PM_{2.5}}) \\
&= log(u_{d,t}) + \Delta C_{d,t,PM_{2.5}} \beta_{PM_{2.5}}.
\end{aligned}
$$

Next we take the exponential of both sides, which gives an expression for the predicted new mortality rate after perturbing concentrations of $PM_{2.5}$,

$$u^*_{d,t} = u_{d,t}exp(\Delta C_{d,t,PM_{2.5}}\beta_{PM_{2.5}}).$$

We then calculate the change in expected mortality rate from the non-perturbed base-case, which gives the change in mortality rate,

$$\begin{aligned}
\Delta u_{d,t} &= u^*_{d,t} - u_{d,t} \\
\Delta u_{d,t} &= u_{d,t}exp(\Delta C_{d,t,PM_{2.5}PM_{2.5}}) - u_{d,t} \\
&= u_{d,t}(exp(\Delta C_{d,t,PM_{2.5}}\beta_{PM_{2.5}}) - 1).
\end{aligned}$$

Finally, because the argument in the exponential, $\Delta C_{(d,t,PM_{2.5})}\ \beta_{(PM_{2.5})}$ is assumed to be small, we use the constant and linear term of the Taylor series approximation of $exp(x)$,

$$exp(x) - 1 \approx x, \text{ for small x}$$

which when simplified gives the final linearized approximation,

$$\Delta u_{d,t} \approx u_{d,t}\Delta C_{d,t,PM_{2.5}}\beta_{PM_{2.5}}.$$

The final approximation is a linearized prediction of the change in mortality rate $\Delta u_{d,t}$ due to a change in pollutant concentration given by $\Delta C_{(d,t,PM_{2.5})}$. The approximation is dependent on the observed base case mortality rate $u_{d,t}$, and the log-relative rate of increase in mortality rate due to an increase in $PM_{2.5}$ concentration, $\beta_{(PM_{2.5})}$.

Note that for our application, because the change in average concentration across the month is relatively small, the linearized approximation is appropriate. For larger deviations, however, the sensitivities and the approximation will both have larger non-linear terms and will have a multiplicative error in approximation. In such cases, new sensitivities should be generated to better reflect the larger changes in emissions.

We use this linearized approximation in our unit commitment model to examine how health impacts change due to a change in pollutant concentration for the state of Georgia. The final form that appears in our objective function is also dependent on time (each hour) as above and on space (each grid square). When we estimate pollutant concentration, the concentration is assumed to be the same at all points within a grid square, with all population exposed uniformly within the grid square.

3.5 Extended results

In addition to results for July from each year, we report separate results for January in Table 3. For the all the years studied, January production costs are negligibly different between the two scenarios relative to the total of health impact costs and production costs, due to the difference being within the optimality guarantee of our solver (set at 0.25% of total cost).

3.5.1 Hourly fuel use differences plot by year

July fuel use difference plots for 2004-2011 are shown in Fig. 10 and Fig. 11, and are dependent primarily the fuel cost ($ / MWh) differences between coal and natural gas. In years where coal was cheaper than natural gas (such as 2004), there are large reductions in coal use possible due to the higher use of coal, and thus larger health impact differences. In years where coal was more expensive than natural gas (such as 2009), coal is used sparingly due to the cheap availability of natural gas, and thus there are smaller health impact differences.

To validate our choice of baseline model which takes into account production which minimizes production cost, we compared our loads for coal, gas, and oil production, which were each tracked at the plant level hourly by the EPA via CEM July 2007 with labels from the EPA eGRID 2007 database [38]. Because July 2007 was used in generating the summer air quality sensitivities, we used July 2007 as a comparison. Nuclear, Hydro and Biomass were not comparable in July 2007, as these plants are

Table 3: January monetized difference in health impacts (health costs), increased production costs and avoided deaths when minimizing the sum of production costs and monetized health impacts, versus minimizing production costs. Percentage of health impact decrease and percentage of production cost increase is given in parentheses. Note that the differences in production cost are less than the tolerance of the optimization model (0.25%).

	in millions USD2007			
Year	**Health Impact Decrease**	**Production Cost Increase**	**Est. Lives Saved**	**January Total Generation (GWh)**
2004	$1.7 (14.7%)	$0.36 (0.1%)	0.2	10,585
2005	$2.4 (22.7%)	$-0.19 (-0.1%)	0.3	9,735
2006	$2.2 (18.9%)	$0.00 (0.0%)	0.3	9,989
2007	$2.0 (13.6%)	$0.44 (0.1%)	0.3	11,511
2008	$1.9 (14.4%)	$0.27 (0.1%)	0.2	12,063
2009	$0.1 (2.0%)	$-0.08 (0.0%)	0.0	10,823
2010	$1.3 (32.8%)	$0.11 (0.0%)	0.2	11,551
2011	$0.1 (3.4%)	$-0.14 (0.0%)	0.0	11,195
Totals	$11.6 (16.5%)	$0.77 (0.0%)	1.5	87,452

not necessarily equipped with hourly emissions monitoring systems by the EPA.

Table 4 illustrates how at the monthly level the modeled coal power generation is comparable to generation loads as recorded by EPA CEM for July 2007. Our model differs in natural gas production, in part due to assumed loads at hydro generating and nuclear generating plants, which are not recorded by EPA CEM. We do not believe this substantially alters results, but could skew health savings impacts higher due to the possibility for more natural gas replacement potential over what was historically possible. Although coal and natural gas are comparable in monthly load, at the plant level and hourly level of detail it is much more difficult to validate each generating unit. In our model, many coal power plants are near substitutes. But in reality, there may be strategic operational differences where a power company may choose to operate one plant of the same fuel type or different fuel type over e.g., another plant. These include pipeline availability of natural gas, transmission constraints when substituting a natural gas plant far away from demand with a coal powered plant near demand.

3.5.2 Comparison of temporally resolved pollutant formation versus a non-temporal averaged pollutant formation

To validate the impact of temporal formation of pollutants on the model, we ran the model under two scenarios, a new scenario using a non-temporally dependent averaged pollutant formation for each grid square and point-source combination, and a scenario

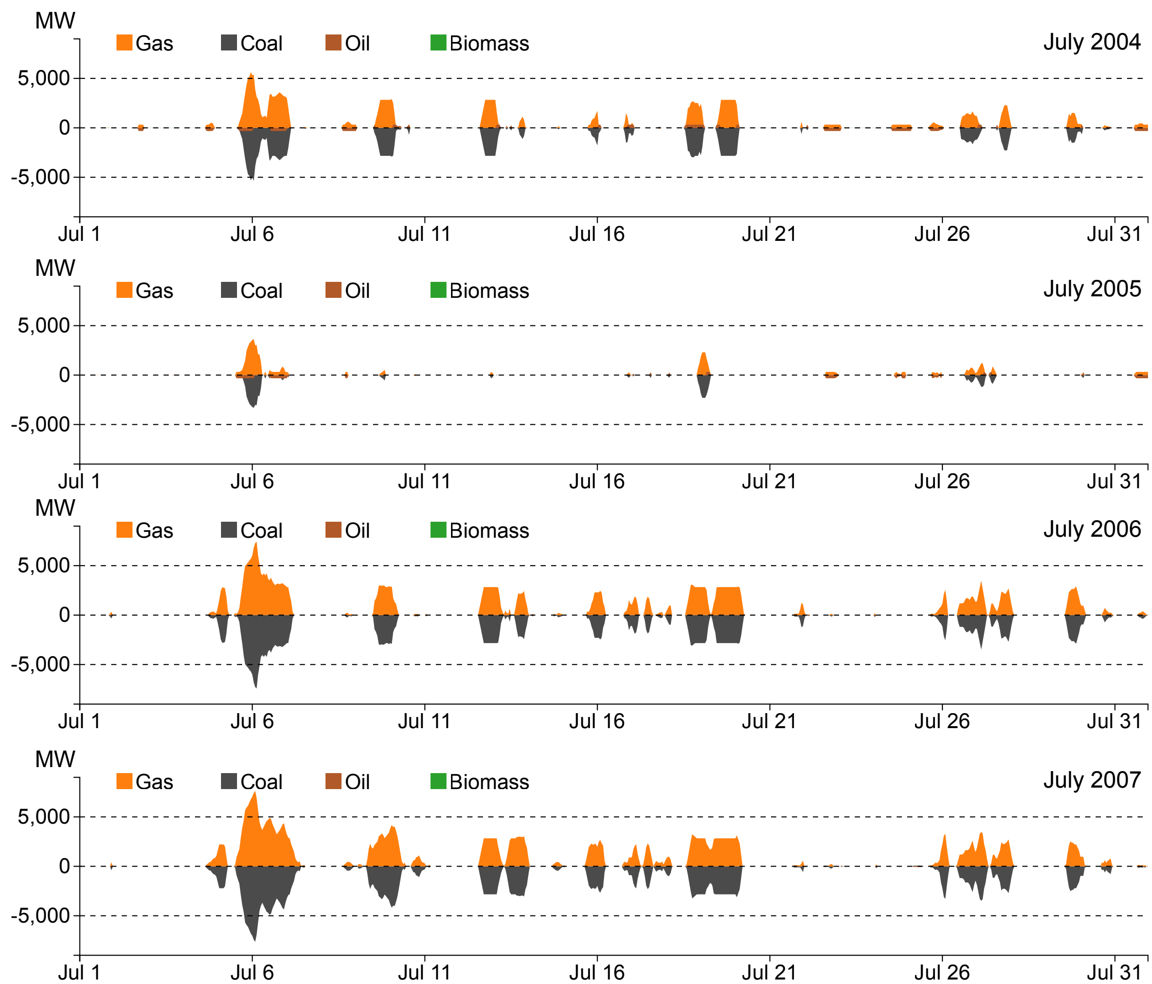

Figure 10: July 2004 through 2007 hourly difference in fuel use in scenario minimizing both production cost and monetized health impacts and the scenario minimizing production cost. Positive values indicate more of that fuel being used in the scenario including health impacts. A value of 0 indicates no change during that hourly period between the two scenarios. Nuclear and hydro do not change between the two scenarios, so they are not shown.

using the temporally resolved pollutant formation. The temporal resolution allowed for an increase in approximately 12.3 additional lives saved over the years of 2004 to 2011 when compared to the model without temporally resolved pollutant formation using a \$6.2M USD_{2007} VSL. Using a \$7.61M USD_{2007} VSL, there was approximately 14.9 additional lives saved over the years of 2004 to 2011 when compared to the model without temporally resolved pollutant formation. These results are shown in Table 5 and Table 6.

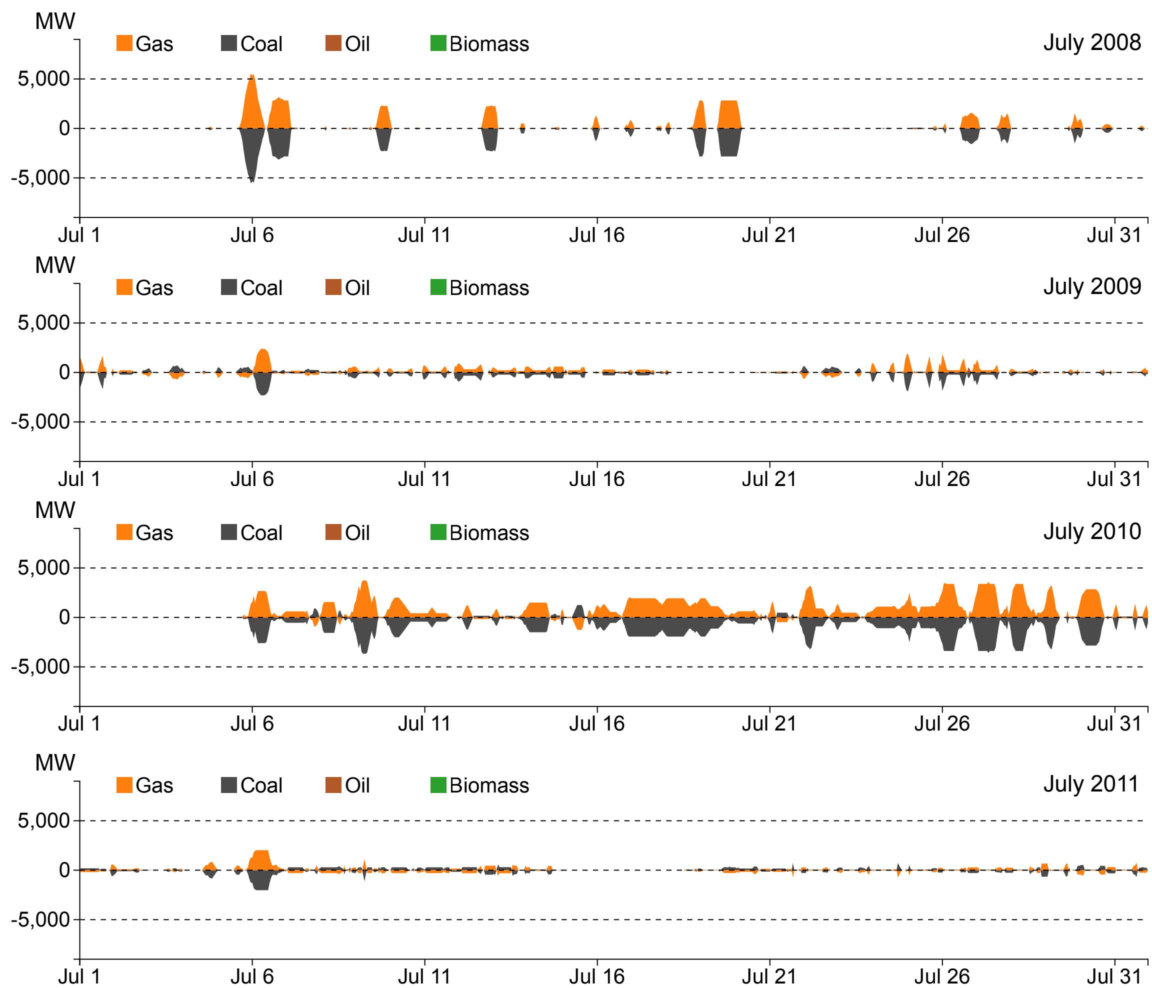

Figure 11: July 2008 through July 2011 hourly difference in fuel use in scenario minimizing both production cost and monetized health impacts and the scenario minimizing production cost. Positive values indicate more of that fuel being used in the scenario including health impacts. A value of 0 indicates no change during that hourly period between the two scenarios. Note that nuclear and hydro do not change between the two scenarios, so they are not shown.

Table 4: Generation load in the unit commitment optimization model minimizing production cost without health impacts, versus actual generation as recorded by EPA CEM for Coal and Natural Gas plants in July 2007.

	July 2007 Generation (GWh)	
	Model Minimizing Production Cost	**Generation as Recorded by EPA CEM**
Coal	8,684	8,689
Natural Gas	1,174	1,717

Table 5: Using a \$6.2M USD_{2007} VSL, additional avoided deaths when comparing the use of average pollutant formation versus temporally-resolved pollutant formation.

Year	**Avoided Deaths with Average Pollutant Formation**	**Additional Lives Saved with Hourly Resolved Pollutant Formation**	**Total Estimated Avoided Deaths**
2004	0.8	2.3	3.1
2005	0.4	0.9	1.3
2006	0.7	3.1	3.8
2007	0.7	3.4	4.1
2008	0.7	1.9	2.6
2009	0.4	0.4	0.8
2010	2.9	-0.1*	2.8
2011	0.5	0.3	0.8
Total	**7.0**	**12.3**	**19.3**

*Due to the use of an 0.25% optimality gap tolerance, these values are within the expected modeling error.

3.5.3 Comparison of spatial resolution by county versus 12 km grid

APOM uses a higher spatial resolution than previous models such as APEEP [24] which uses county-level resolution. Because there are 154 counties in Georgia, and APOM uses roughly 1,100 grid squares, there are on average 7.5 grid squares per county, or nearly an order of a magnitude increase in spatial resolution. To illustrate the impact of the higher spatial resolution, the average health impacts from Plant Bowen for July 2007 are plotted in Figure 12 for Bartow County in Georgia. APOM utilizes a 12 km grid, and replaces Bartow County with 16 grid squares. These grid

Table 6: Using a \$7.61M USD_{2007} VSL, additional avoided deaths when comparing the use of average pollutant formation versus temporally-resolved pollutant formation.

Year	Avoided Deaths with Average Pollutant Formation	Additional Lives Saved with Hourly Resolved Pollutant Formation	Total Estimated Avoided Deaths
2004	0.7	2.7	3.4
2005	0.5	1.0	1.5
2006	0.7	4.1	4.8
2007	0.7	4.5	5.2
2008	0.7	2.5	3.2
2009	0.4	0.3	0.7
2010	3.3	-0.2*	3.1
2011	1.0	0.2	1.2
Total	**8.2**	**14.9**	**23.1**

*Due to the use of an 0.25% optimality gap tolerance, these values are within the expected modeling error.

squares have varying health impacts as shown in Figure 12. These health impacts vary from \$3.32 per month per person to \$18.79 per month per person (July 2007, USD_{2007}) illustrating heterogeneous intra-county impacts. Using an average value of \$8.04 per person would under- or over-value health impacts within these grid squares.

3.5.4 Sensitivity analysis

Fig. 13 and Fig. 14 illustrate the sensitivity of model results of lives saved to five VSL estimates (min, 25th percentile, median, 75th percentile and max) from the 26 EPA reference studies (see Table 33). Results are shown for each VSL estimate, for 25 random samples of $\beta_{PM_{2.5}}$, the measured causal link between $PM_{2.5}$ concentration and increased mortality. The 25 samples of $\beta_{PM_{2.5}}$ are generated using a normal distribution with mean all-cause mortality increase of 5.8% per 10 μg/m^3 change in ambient $PM_{2.5}$ concentration [38], and a standard deviation of 2.16% per 10 μg/m^3 [28].

In addition to sulfate-based $PM_{2.5}$ formed from SO_2 emissions, we analyzed sensitivities of ozone and $PM_{2.5}$ formation downwind of generating units due to NO_X emissions and the resultant monetized health impacts through increased mortality. In particular, $PM_{2.5}$ formation from NO_X emissions was the next largest health impact pollutant, but was roughly an order of magnitude less than sulfate-based $PM_{2.5}$ due to SO_2 emissions. Although for our case study we only considered SO_2 emissions forming sulfate based $PM_{2.5}$, the methodology and CMAQ DDM-3D is capable of generating the sensitivities from these other emissions and pollutants including ozone and species of $PM_{2.5}$.

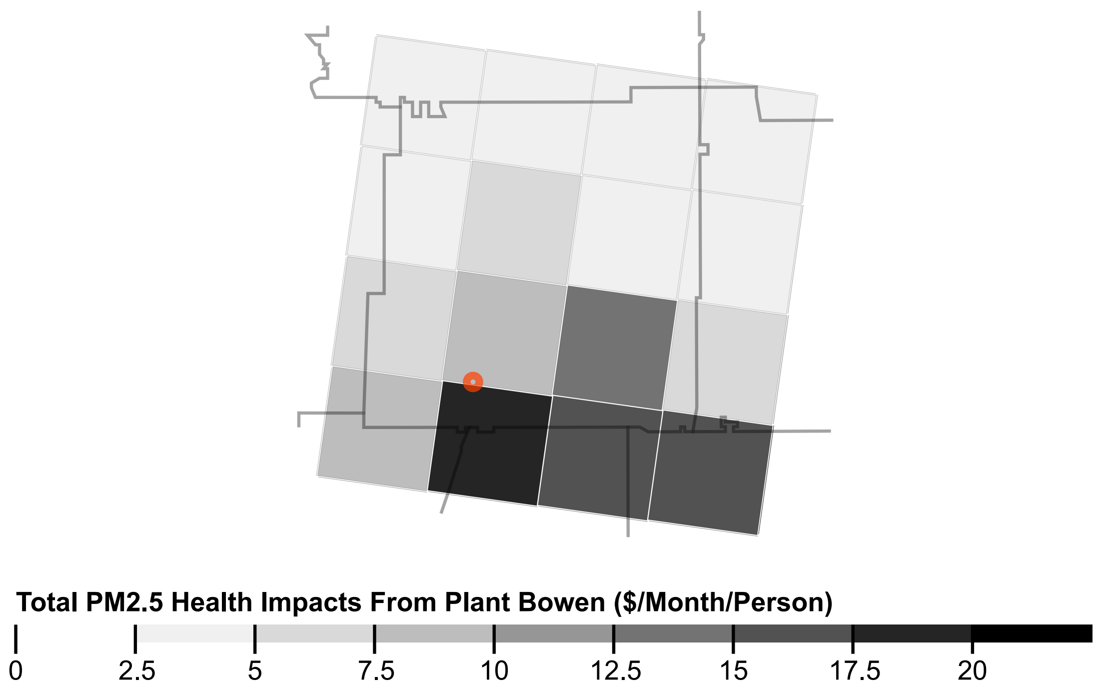

Figure 12: July 2007 Bartow County health impacts from Plant Bowen due to sulfate-based $PM_{2.5}$. Previous modeling efforts such as APEEP [24] provide average results over the whole county. The figure shows the higher resolution results with the 12 km grid of the APOM model overlaying the map of Bartow County, with Plant Bowen shown as a red dot.

3.5.5 CMAQ DDM-3D performance metrics

The model performance is evaluated using air quality system (AQS) observational data. The performance metrics for 8-hour average O_3 and 24-hour average $PM_{2.5}$ concentrations for the modeling domain are summarized in Table 7, and they are near the acceptable range according to the guidance by [3].

3.5.6 APOM model implementation

The original implementation of DDM-3D can be found in Yang et al., (24), with the addition of the ability to capture particulate matter sensitivities in Boylan et al., [2] and Zhang et al. [49]. DDM-3D in CMAQ is now included in the standard versions of CMAQ and is widely used for scientific studies as well as by the US EPA for regulatory analysis [30]. The details of using DDM-3D in constructing a reduced form model to efficiently provide the impact of controls is found in Cohan et al. [8].

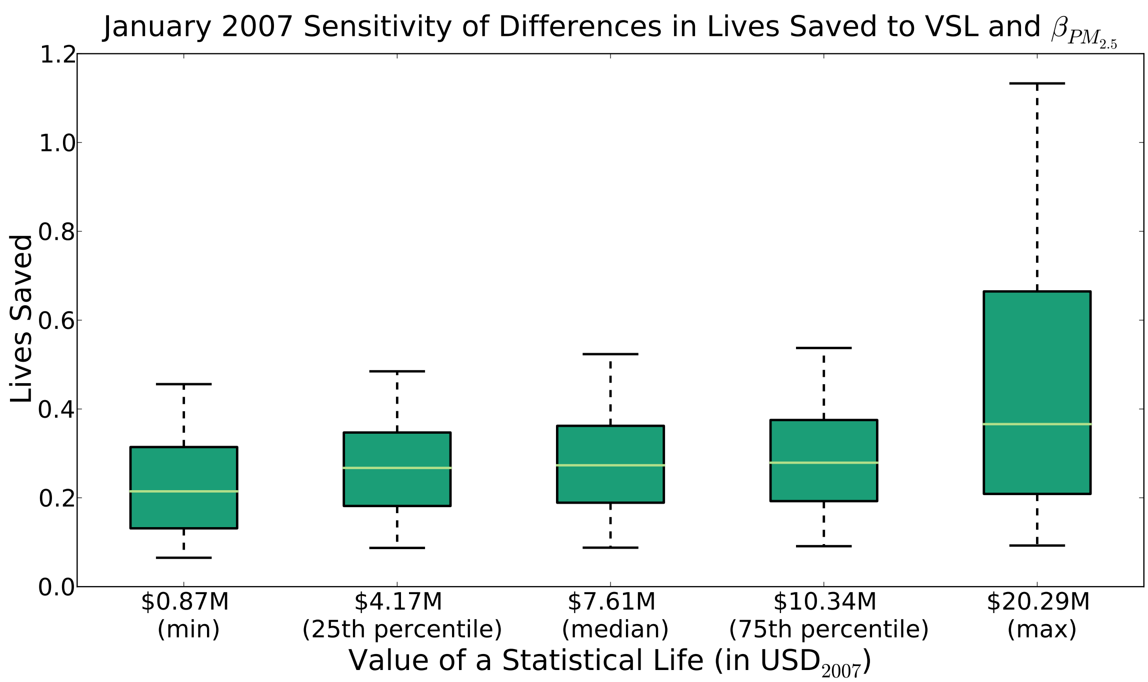

Figure 13: January 2007 lives saved in the scenario including health impacts vs. scenario not including health impacts. Shown are results from 25 samples of $\beta_{PM_{2.5}}$, for five values of statistical life (VSL) estimates; the minimum, the 25th, 50th and 75th percentile estimates and the max from 26 EPA VSL studies listed in Table 33

Table 7: Performance metrics for 8-hour average ozone concentrations and 24-hour average $PM_{2.5}$ concentrations

Pollutants	**Months**	**Mean Bias**	**Mean Error**	**Normalized Mean Bias (%)**	**Normalized Mean Error (%)**
Ozone	January	-1.04 ppb	6.88 ppb	-5.39	35.7
	July	6.49 ppb	12.58 ppb	20.29	39.36
$PM_{2.5}$	January	3.30 μg m^{-3}	4.94 μg m^{-3}	32.63	48.88
	July	-1.67 μg m^{-3}	5.09 μg m^{-3}	-11.61	35.37

The optimization component of APOM is given in Section 3.2. The equation from Section 2.4.2 is used outside of the optimization for the reconstruction of concentrations due to perturbed emissions profiles. For example, the equation in Section 2.4.2 is used to compute the estimated concentration of $PM_{2.5}$ given a perturbed emissions

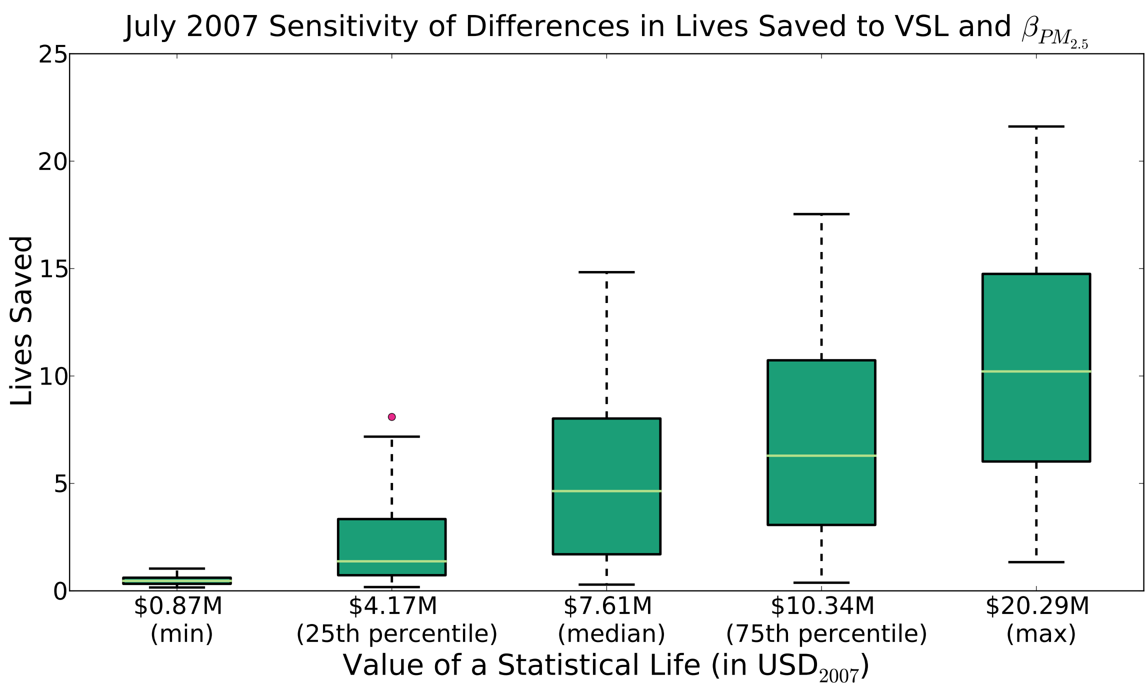

Figure 14: July 2007 lives saved in the scenario including health impacts vs. scenario not including health impacts. Shown are results from 25 samples of $\beta_{PM_{2.5}}$, for five values of statistical life (VSL) estimates; the minimum, the 25th, 50th and 75th percentile estimates and the max from 26 EPA VSL studies listed in Table 33

profile at a given hour and location. Input files used to generate the DDM fields, as well as the output sensitivity coefficients and other APOM files are all available on request at http://www.APOM.gatech.edu.

CHAPTER IV

DEMOGRAPHIC ANALYSIS OF HEALTH IMPACTS DUE TO REDUCTIONS IN ELECTRICITY GENERATION EMISSIONS

There have been large reductions in electricity generation unit SO_2 emissions in the US state of Georgia over the years of 2007 to 2015. These emissions changes have reduced $PM_{2.5}$ air pollutant concentrations and have had many positive impacts on affected populations. However, previous research has not quantified the specific impacts of pollutant control technology and fuel switches from coal to natural gas using a temporal dimension of analysis and a high spatial resolution. We estimate the positive impacts by individual electricity generation source and compare those benefits across races. These benefits are estimated for the one month period of July 2015 vs. July 2007 illustrating a reduction in monetary health impacts of $763 million 2007 US dollars or 100 lives saved.

4.1 Introduction

Poor air quality has been linked to problematic health and environmental concerns [28]. These problems have costly impacts and can be prevented via a switch to cleaner fuels or electricity generation types, pollutant control technologies that capture emissions, or a modified generation schedule that avoids harmful emissions during specific predictable poor air quality time periods where wind blows pollutants towards highly populated areas [28].

Optimization models of air pollution and controllable anthropogenic sources such as electricity generation units depend on several interdependent linkages [18]. These linkages are models of emissions and atmospheric chemistry which estimate air pollutant concentrations at a fine spatial and temporal resolution, air pollutant concentration health and damage impacts, valuation of these impacts and an optimization model which can trade-off the cost of reducing emissions in specific locations and the cost of health impacts if those emissions are not reduced [18].

Mathematical modeling of air pollution has a long history within the study of atmospheric chemistry, spanning several iterations of models which have improved in both geospatial and temporal resolution [4]. These models have recently been used to create day-ahead predictive models of air pollution [17]. Day-ahead models allow sufficient planning horizons for turning on and off air pollution sources when wind and weather conditions blow air pollution towards high-density populations causing adverse impacts on residents in these areas [18].

Modeling of air pollution can be linked with damage estimation creating the quantity of adverse impacts used in cost valuation. These damage estimates have improved over time, and use log-likelihood regression and other math models to estimate the impact of air pollutant concentrations on mortality, emergency room visits, asthma incidence and a variety of other health and environmental impacts [28],[22].

The predominant damage from air pollutants via a dollar valuation perspective is increased mortality rates [22]. Valuation of these deaths and increases in mortality is difficult, and typically is done with survey methods [39]. The United States Environmental Protection Agency (US EPA) compiled a 27 study estimation, and recommended a valuation method for increased mortality with a median value of \$7.61 million per life (adjusted to USD_{2007} using US GDP deflators) [39].

The key to many of the air quality concentration models is sensitivity estimation of air pollutant concentrations to changes in emissions at point sources. One version in wide use is the Community Multiscale Air Quality model, or CMAQ [4]. The sensitivity package is the Direct Decoupled Model in three Dimensions or CMAQ

DDM3D [49].

Regional case studies have explored these linkages across the globe in areas such as South Korea and Georgia. These case studies have demonstrated the large impact of modified emissions controls [19],[18].

There has not been a study of extensive simultaneous air quality sensors covering an area at consistent grid spacing throughout the world, so modeling is necessary to estimate the air quality in a specific area [3]. There are sensors, however, which cover an area, and can be used to test these modeling results [49]. However, the true exposure experienced by a human or animal may differ from either the modeled or measured impact at nearby air quality stations. That unknown exposure presents an issue in estimating pollutant concentrations exposed to a population. This can be partially resolved by taking both measurements and modeling into account when evaluating health impacts. For the purposes of this thesis, we focus on modeling of air quality concentrations, and not on the validation of those models due to these aforementioned difficulties. That should not deter future research into this area.

Environmental justice measures or evaluating equity is key when evaluating policy changes that impact reductions in emissions from some areas but not others [47]. In this paper we measure how reductions in emissions impact local pollutant levels and environmental justice measures after implementation of air quality regulations such as the EPA cross-state air pollutant rule [44]. Because air quality monitors are not stationed at every household across the country and cannot differentiate among source emissions impacts, air quality models play an important role in estimating the impacts of emissions reductions on pollutant concentrations [3].

In our study we examine the regulated air pollutant fine particulate matter ($PM_{2.5}$) and the resultant reductions due to decreases in SO_2 emissions at plants within the state of Georgia. There was an 96% reduction in SO_2 emissions from electricity generating units in Georgia between July 2007 and July 2015 (see Fig. 15) from a variety of factors, including emissions control technologies installed during that timeframe as well as shifts from coal-fueled generation to natural gas fueled generation [45]. Within Georgia, future reductions due to nuclear units coming online in 2019 will drive additional reductions due to the shutdown of plants burning fuels such as coal, natural gas and variants of biomass.

Figure 15: July 2007-2015 Georgia electricity generating unit year-over-year decreases in SO_2 emissions, in thousands of lbs.

Previous analyses have examined $PM_{2.5}$ reductions and changes in mortality using air quality monitor station data. These are limited by monitor characteristics such as the lack of geospatial density and the specific locations and heights chosen. Air quality monitoring is thus limited in spatial resolution and historical estimates where monitors did not previously exist. Additionally apportionment is not possible using air quality monitors and further makes assessing specific-plant-level impacts difficult. Air quality modeling is then a necessity for assessing source-level impacts and a high spatial resolution.

Alternative air quality modeling with spatial and source apportionment have examined population based impacts. We build on those results providing time-of-day impacts, maximum hour exposure estimates and a sensitivity analysis of our results to geospatial imprecision.

We outline an environmental justice perspective driven by these SO_2 reductions, examining race-and origin-based measures of exposure to $PM_{2.5}$. Examining environmental justice estimated impacts illustrates the wide ranging impacts across race and origin that may influence the impact that new regulations have had on different population groups.

We explore two research questions in this manuscript. First, we evaluate the health impacts by electricity generating unit due to the installation of pollutant control technology and due to the switch from coal to natural gas. We find significant impacts of roughly $763M annually when using July 2015 emissions in July 2007 instead of July 2007 emissions. This helps quantify the large potential benefits of large capital expenditures on pollutant control technology and fuel switches from coal to natural gas. Second, we compare the impacts across race/origin to examine the heterogeneity in impacts.

4.2 Methodology

The model is summarized in Figure 16. We use an air quality model estimating the impacts of decreased emissions from point sources within Georgia in July 2015 vs. July 2007 emissions, with an air quality modeling period from 2007. This allows us to quantify the health impacts of lowered emissions using July 2015 technology in July 2007. US Census estimated population demographics are used from 2010, with adjusted population for each year from 2007-2009 and 2011-2015 based on the change in Georgias population. The connection between decreased all-cause mortality rates and decreased pollutant concentrations of fine particulate matter ($PM_{2.5}$) was from Pope et. al [28].

In Table 8 the estimated proportion of population responding to race in the US Census 2010 questionnaire for the single choices of White, Black or African American, and several other races are shown. Additionally 2.14% responded with two or more races. An additional question asks about Hispanic/Latino origin with roughly 8.81% of respondents. The questions from the 2010 US Census are seen in Fig. 17.

In Table 9 we see the estimated reduction in SO_2 emissions per MWh of production using EPA CEM data. Plant Bowen and Scherer have both had SO_2 scrubbers installed which lower their emissions of SO_2 per MWh substantially. Plant McDonough located northwest of Atlanta had a substantial drop in emissions of SO_2 when switching to natural gas combustion from coal even with an increase in generating capacity.

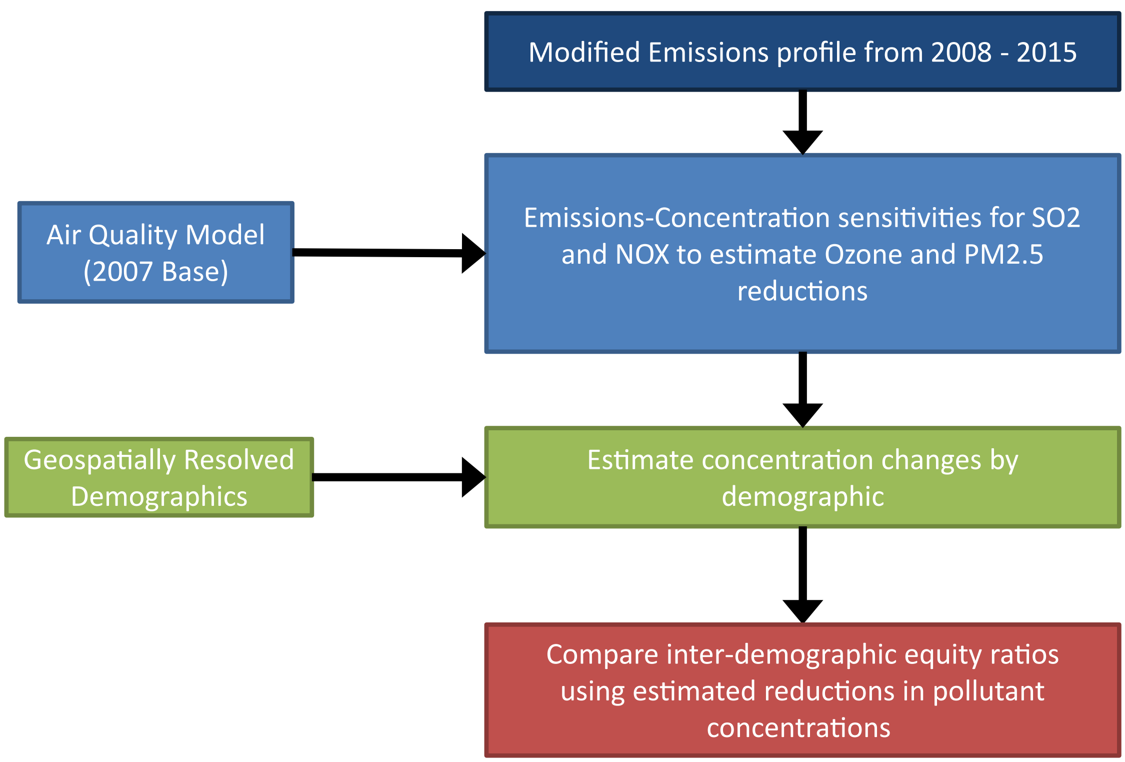

Figure 16: Health impact valuation process across geospatially resolved demographics

Table 8: Answers regarding race or Hispanic/Latino origin in Georgia from the 2010 US Census

	Georgia US Census Race or Hispanic/Latino
Single Choice - Total	97.86%
White	59.74%
Black	30.46%
Other Race	4.01%
Asian	3.25%
Two or more races	2.14%
Hispanic or Latino Origin	8.81%

In Table 10 we see the GWh of production for the month of July for each plant. McDonough had large upgrades to capacity from 2007 to 2015 when switching to natural gas. Both Bowen and Scherer maintained similar capacity between 2007 and 2015.

In Table 11 we see the emissions in millions of pounds of SO_2 from each plant.

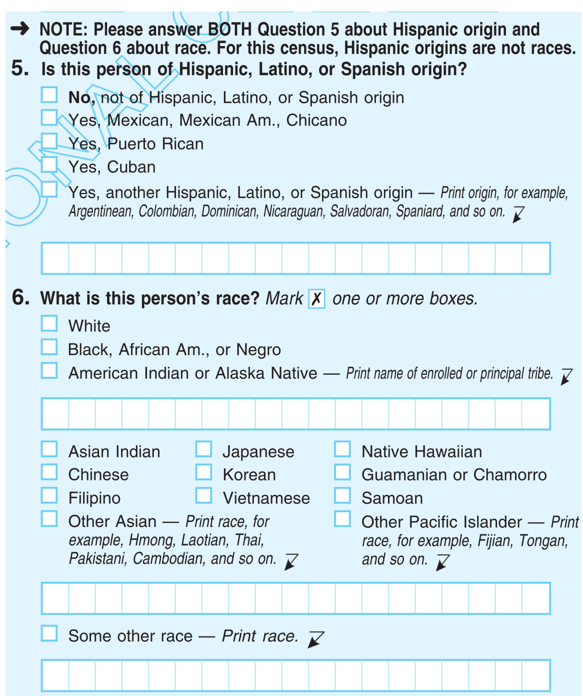
→ NOTE: Please answer BOTH Question 5 about Hispanic origin and Question 6 about race. For this census, Hispanic origins are not races.

5. Is this person of Hispanic, Latino, or Spanish origin?
- ☐ No, not of Hispanic, Latino, or Spanish origin
- ☐ Yes, Mexican, Mexican Am., Chicano
- ☐ Yes, Puerto Rican
- ☐ Yes, Cuban
- ☐ Yes, another Hispanic, Latino, or Spanish origin — *Print origin, for example, Argentinean, Colombian, Dominican, Nicaraguan, Salvadoran, Spaniard, and so on.*

6. What is this person's race? *Mark ✗ one or more boxes.*
- ☐ White
- ☐ Black, African Am., or Negro
- ☐ American Indian or Alaska Native — *Print name of enrolled or principal tribe.*
- ☐ Asian Indian
- ☐ Chinese
- ☐ Filipino
- ☐ Other Asian — *Print race, for example, Hmong, Laotian, Thai, Pakistani, Cambodian, and so on.*
- ☐ Japanese
- ☐ Korean
- ☐ Vietnamese
- ☐ Native Hawaiian
- ☐ Guamanian or Chamorro
- ☐ Samoan
- ☐ Other Pacific Islander — *Print race, for example, Fijian, Tongan, and so on.*
- ☐ Some other race — *Print race.*

Figure 17: Questions on Race and Latino/Hispanic Origin from the 2010 US Census

Table 9: SO_2 emissions rate comparison between July 2007 and July 2015 across three power plants in Georgia

	SO_2 Emissions Rate (lbs / MWh)		Reduction in SO_2
Plant	**July 2007**	**July 2015**	**Emissions Rate**
Bowen	15.3	1.1	93%
McDonough	14	0.0	100%
Scherer	5.8	0.1	98%

Table 10: Power production comparison between July 2007 and July 2015 across three power plants in Georgia

	GWh Production	
Plant	**July 2007**	**July 2015**
Bowen	2,263	1,883
McDonough	349	1,628
Scherer	2,311	2,016

There is at least one order of magnitude of reduction in SO_2 emissions from each plant studied over the month of July in 2015 vs. 2007.

4.3 Results

For the largest demographic populations we studied the estimated improvement in $PM_{2.5}$ concentration and exposure in the month of July. We compared 2007 to 2015 using the estimated reduction in SO_2 emissions by hour of day to estimate the reduction in sulfate SO_2-based $PM_{2.5}$ exposure by population on a 12km-by-12km grid.

Table 11: Total SO_2 emissions comparison between July 2007 and July 2015 across three power plants in Georgia

	SO_2 Emissions (000,000 lbs)	
Plant	**July 2007**	**July 2015**
Bowen	34.6	2.0
McDonough	4.9	0.0
Scherer	13.4	0.2

Table 12: Georgia population estimates (Ages 30+) using answers to 2010 US Census questions

	White	**Black**	**Other**	**Hispanic/Latino**
Pop. Estimate (Ages 30+)	3,502K	1,717K	551K	492K

Table 13: $PM_{2.5}$ Improvement (μg/m^3) by power plant and race, with a 3x3 grid square sensitivity

	White	**Black**	**Other**	**Hispanic/Latino**
Average $PM_{2.5}$ improvement [Min,Max] in a nine (3x3) grid square sensitivity				
Bowen	0.218 [0.211,0.221]	0.152 [0.147,0.154]	0.269 [0.260,0.269]	0.26 [0.258,0.262]
Scherer	0.034 [0.032,0.035]	0.038 [0.035,0.039]	0.034 [0.0323,0.036]	0.034 [0.033,0.035]
McDonough	0.022 [0.022,0.023]	0.0293 [0.029,0.030]	0.0316 [0.031,0.032]	0.0305 [0.030,0.031]

The results for three high emissions power plants are shown in Table 13. Note that on an aggregate or total SO_2 emitted basis, Bowen saw the largest improvements. Although Scherer also had large reductions in SO_2 emissions, the location further away from populated areas such as Atlanta, Georgia led to less substantial improvements on a geospatially-averaged and population-affected basis. Examining hour-by-hour data however there are still substantial improvements in estimated air quality impact.

Table 13 also illustrates a sensitivity analysis performed, examining for a given population the 3x3 grid square air pollutant concentrations rather than the single grid square. The analysis allows for uncertainty in the geospatial precision of pollutant concentrations modeled.

In Table 14 we see the resulting improvement in the worst hour of the month from each plant. Note that the average shown in Table 13 underestimates poor air quality hours or days. The reductions due to the switch from coal to natural gas and the installation of SO_2 scrubbers provides a large reduction in worst hour impacts.

Table 14: Worst Hour of the month improvement in $PM_{2.5}$ (μg/m^3) by demographic

	White	Black	Other	Hispanic/Latino
Bowen	5.02	3.89	5.64	5.68
Scherer	0.92	1.08	0.83	0.8
McDonough	0.65	0.96	0.89	0.87

In Figure 18 we see the distribution of average $PM_{2.5}$ estimated improvements by grid square. For Plant Bowen, there are over 5% of grid squares covering over 7000 square km with impact reduction of 0.25 μg /m^3 in $PM_{2.5}$. The distribution of population is skewed to the right, with several large population grid squares seeing a larger decrease in $PM_{2.5}$, in part due to Plant Bowens close proximity to the northwest of the major metropolitan area of Atlanta.

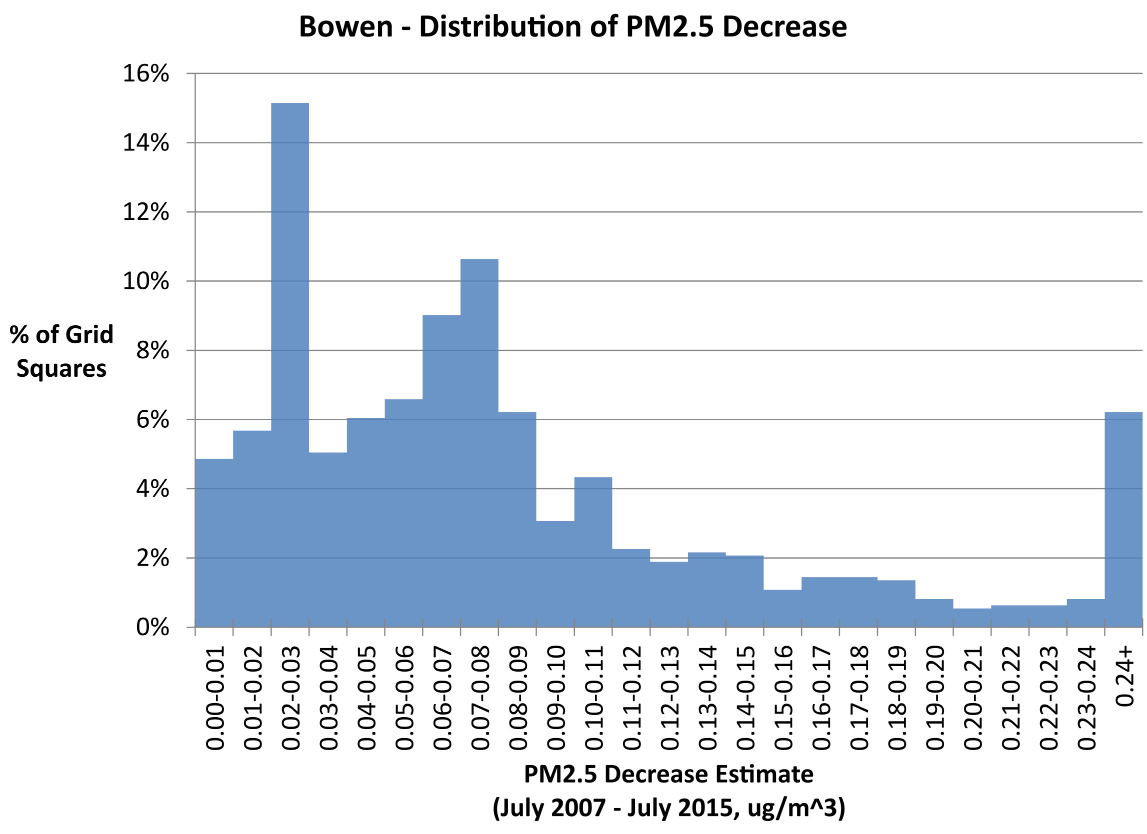

Figure 18: $PM_{2.5}$ decreases from July 2007 to July 2015 due to SO_2 reductions at Plant Bowen

In Figure 22 we see the distribution of $PM_{2.5}$ decreases for Plant Scherer, which has a much shorter tail. The distribution of impacts for Scherer is still substantial with 5% of grid squares or over 7000 square km with impact reduction of 0.08 or more $\mu g/m^3$ in $PM_{2.5}$ improvements.

In Figure 20 we see the impacts of Plant McDonough, which has substantial reductions, but on average the impacts are minor compared to Plant Bowen or Plant Scherer. One of the key impacts of McDonough however is the close nearby dense population in Atlanta, Georgia and the surrounding communities. On poor air quality days the improvements impact a much larger population than Plant Scherer and

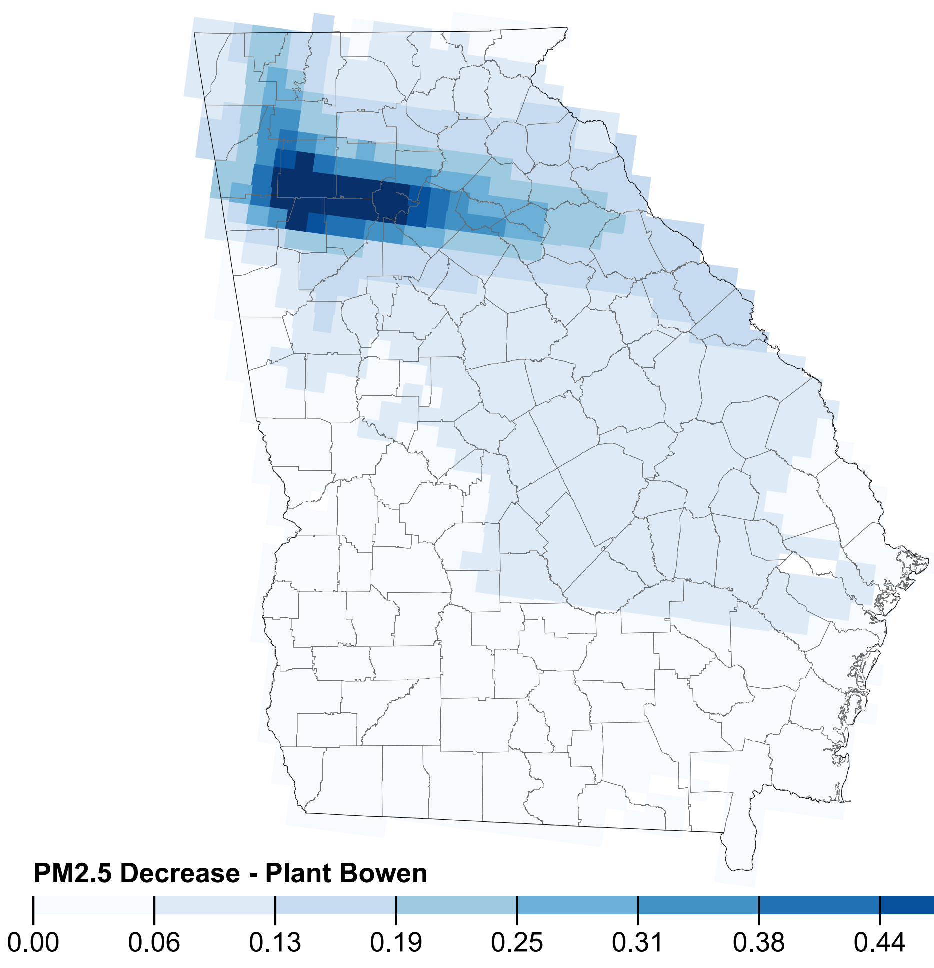

Figure 19: Map of $PM_{2.5}$ decreases from July 2007 to July 2015 due to SO_2 reductions at Plant Bowen

Bowen due to the nearby densely populated areas.

Table 15 shows the model estimates of lives saved from the reduction in $PM_{2.5}$. These reductions vary by demographic population size, so normalized values are shown in Table 16. Table 17 outlines the monetized health impact estimate of these reductions in emissions by plant and demographic, using a VSL of \$7.61M 2007 US dollars.

4.4 Discussion and Conclusion

When policies are implemented without regard to demographic or spatially varying impacts, improvements can be unequal or in the extreme case one group may capture all the improvements at the detriment to others. When potential improvements exist, one environmental justice goal is to evaluate policies that benefit all demographics,

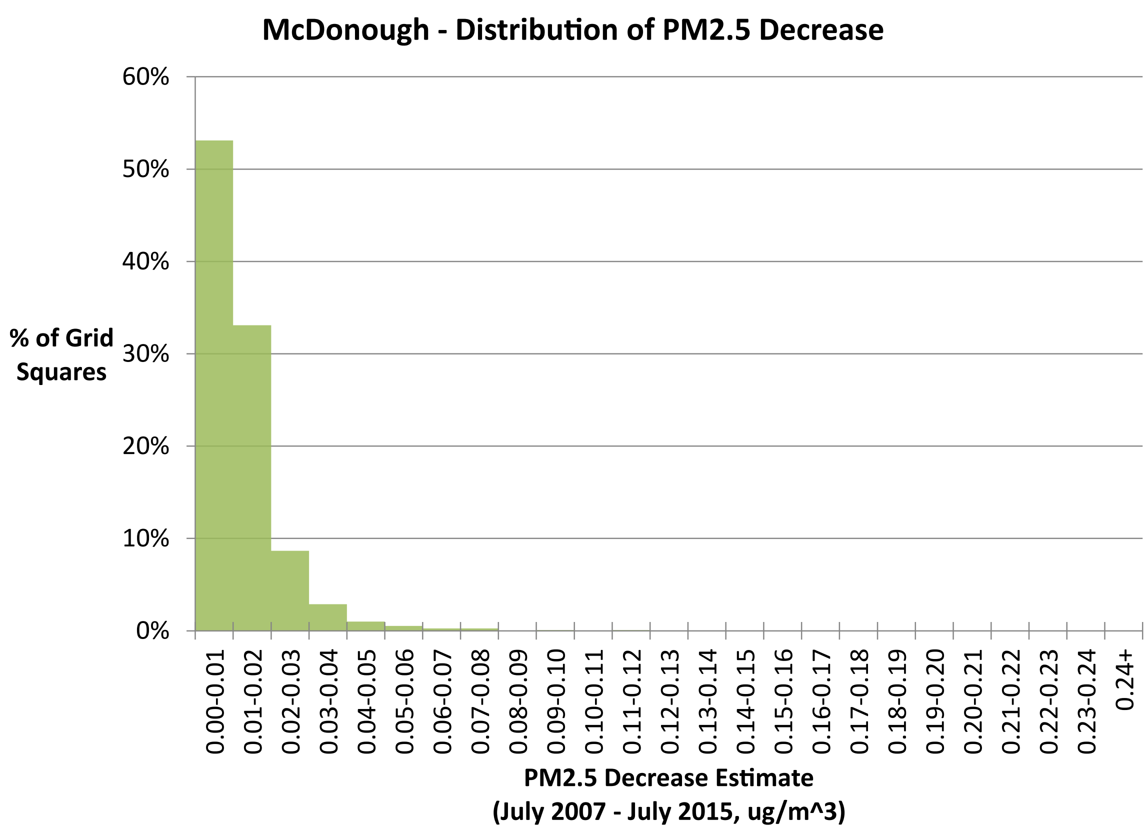

Figure 20: $PM_{2.5}$ decreases from July 2007 to July 2015 due to SO_2 reductions at Plant McDonough

Table 15: Estimated lives saved by demographic when using July 2015 hourly emissions profiles in July 2007

Lives Saved	Total	White	Black	Other	Hispanic/Latino
Bowen	**75.5**	49.8	17.1	8.6	7.7
Scherer	**15.1**	9.0	4.9	1.3	1.1
McDonough	**9.6**	5.3	3.3	1.1	0.9
Total	**100.3**	**64.2**	**25.2**	**11.0**	**9.7**

particularly when implementing new policy.

As a case study presented here, we explore a new tool to evaluate improvements in health impacts on several demographics in Georgia and illustrate improvements across

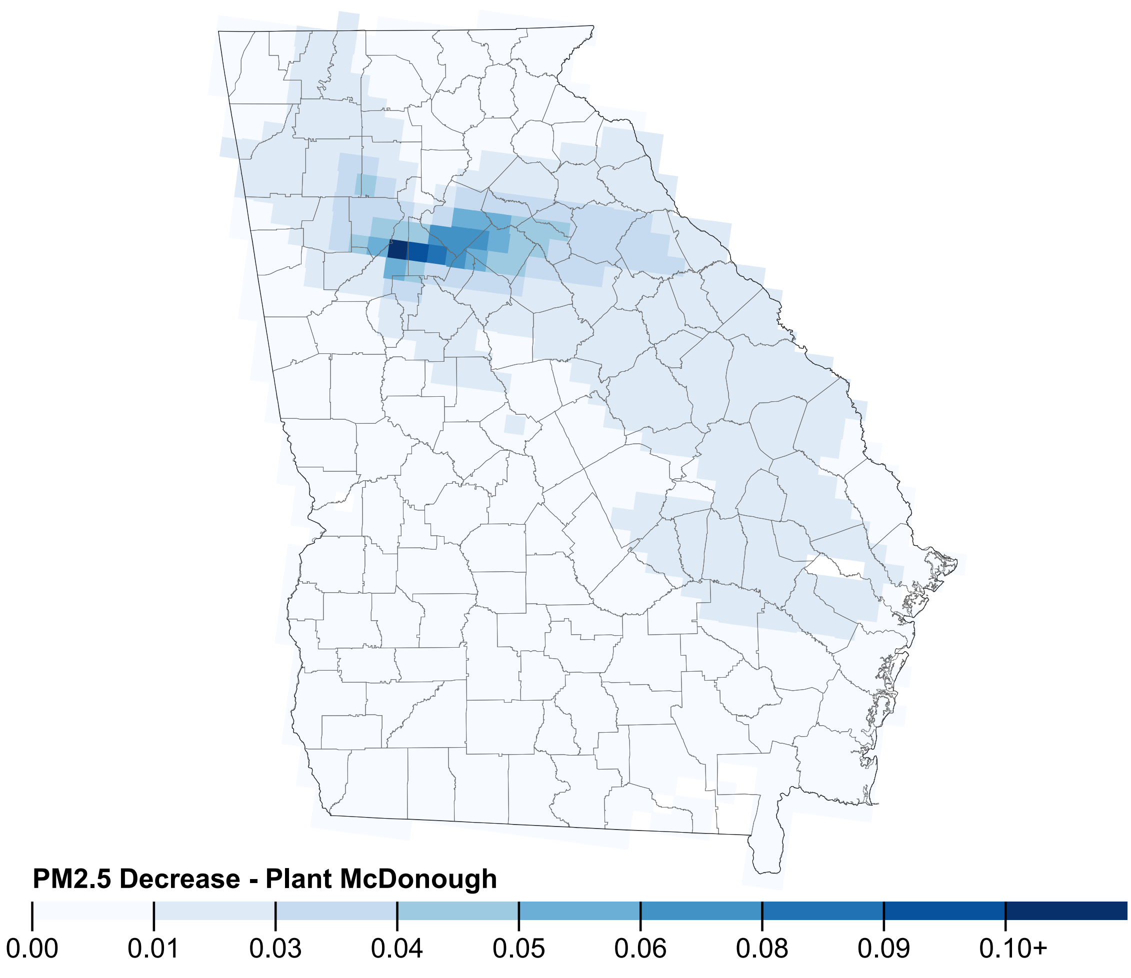

Figure 21: Map of $PM_{2.5}$ decreases from July 2007 to July 2015 due to SO_2 reductions at Plant McDonough

Table 16: Estimated lives saved per 100,000 people by demographic when using July 2015 hourly emissions profiles in July 2007

Lives saved / 100K	Total	White	Black	Other	Hispanic/Latino
Bowen	**1.3**	1.4	1.0	1.6	1.6
Scherer	**0.3**	0.3	0.3	0.2	0.2
McDonough	**0.2**	0.2	0.2	0.2	0.2
Total	**1.7**	**1.8**	**1.5**	**2.0**	**2.0**

each demographic. We use a high spatial resolution air quality model that evaluates point sources individually and varies temporally. This model is in contrast to previous modeling which has not had a temporal dimension combined with a higher spatial resolution. These aspects are key when evaluating impacts across demographics and tracking improvements in worst-case hour air quality improvements.

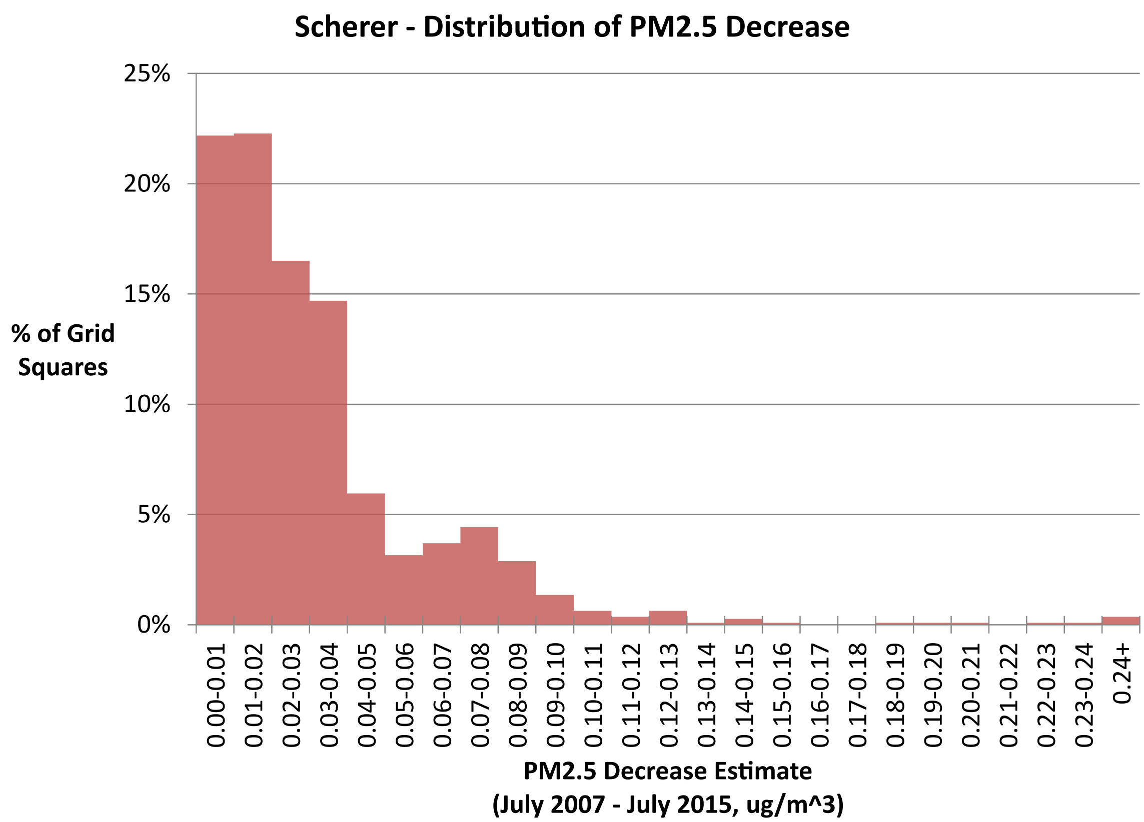

Figure 22: $PM_{2.5}$ decreases from July 2007 to July 2015 due to SO_2 reductions at Plant Scherer

Table 17: Monetized health impacts saved by demographic when using July 2015 hourly emissions profiles in July 2007

$ Impact (Millions)	**Total**	**White**	**Black**	**Other**	**Hispanic/Latino**
Bowen	**$575**	$379	$130	$66	$59
Scherer	**$115**	$68	$37	$10	$8
McDonough	**$73**	$41	$25	$8	$7
Total	**$763**	**$488**	**$192**	**$83**	**$74**

One promising direction of future research is to evaluate and inventory time-varying health impacts of all high emissions point sources such as coal-fired plants across the US. These could be used by local, state and federal government agencies

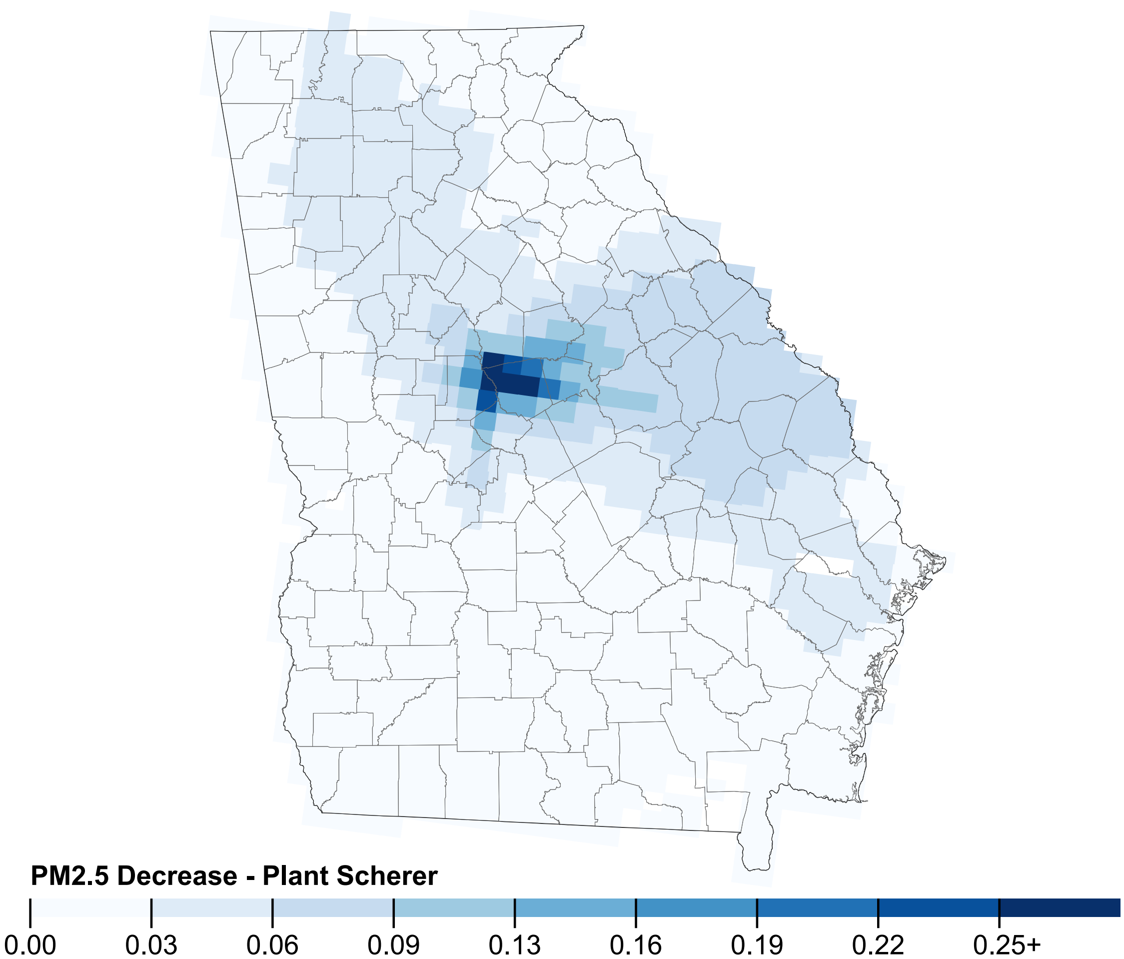

Figure 23: Map of $PM_{2.5}$ decreases from July 2007 to July 2015 due to SO_2 reductions at Plant Scherer

as well as academics to improve policy recommendations of specific emissions sources without the need for each to individually run air quality models. Air quality modeling is hampered or sometimes infeasible due to limited resources and expertise, particularly at the local level. This would be similar to previous models such as APEEP which allow for such analyses but without a temporal dimension of analysis and higher spatial resolution [24].

CHAPTER V

CONCLUSIONS AND FUTURE RESEARCH DIRECTIONS

This thesis newly integrates a reduced form air quality model with time-varying atmospheric impacts within an optimization model. The modeling additionally illuminates several new research directions. These directions are described in what follows, and include potential case studies, theoretical directions and future challenges in the implementation of APOM.

5.1 *Future research directions*

5.1.1 Implementation of APOM

Two steps can bring APOM closer to implementation. The first step is to demonstrate APOM using a daily-generated air quality model. Unlike the retrospective reduced form air quality model presented in Chapter 2, implementation of APOM would require integration of a unit commitment model with a day-ahead reduced form model. A reduced form air quality model can be run on a recurring day-ahead basis similar to [17]. Validating these air quality results over a time period of one or two poor air quality months (e.g. Summer months in Georgia) would illustrate the power of APOM to reduce $PM_{2.5}$ downwind of power plants.

The second step to operationalize APOM is to develop a decision support system to integrate APOM within power systems dispatch. Integration within a current power generation framework in use at a utility (e.g., Southern Company or Georgia Power) would allow testing of the full power of pollutant reduction via generation management.

5.1.2 Case studies using APOM

Although we present a case study of Georgia using APOM in Chapter 2, the method can be applied more generally. One next step is to explore the northeast region of the United States. The northeast region has a combination of both high SO_2 emissions from coal power plants in the Ohio River Valley as well as high population density downwind of these plants. In 2014 there was substantially more SO_2 emitted from coal fired generation in each of six Ohio River Valley states (Ohio, Indiana, Pennsylvania, Kentucky, West Virginia, Illinois) when compared to Georgia (see Table 18, [36]). Four of these states also have higher population density than Georgia (Ohio, Indiana, Pennsylvania and Illinois, see Table 18, [31]). With high population density and high coal-fired SO_2 emissions, applying APOM within these states could identify potential to reduce health impacts. Additionally, analyses in India, China and other countries with high population densities and high emissions could identify opportunities to reduce health impacts. All of these applications in other regions would require development of emissions inventories and electricity system commitment models.

In addition to coupling air quality with power plant unit commitment and dispatch, there are other opportunities to optimize emissions. For example, the refinement of fossil fuels and other manufacturing processes emit harmful pollutants. Those emissions sources can leverage the power of APOM to reduce health impacts on a regional basis.

Substitution of electric power with demand-side management programs such as coordinated decreases in air conditioner usage or decreases in water heater usage can reduce peak generation. These coordinated demand-side programs could improve air quality when applied at specific times recommended by APOM. Integration of demand side management options into the APOM unit commitment could increase its flexibility and power.

Table 18: Top 10 rank of states and Georgia sorted by 2014 annual SO_2 emissions from coal power plants. Population density is shown using July 1, 2014 US Census population estimates.

Rank	**State**	**Coal SO2 Emissions (metric tons)**	**Population Density (pop. per sq. mile)**
1	TX	607,570	103
2	OH	595,660	284
3	IN	537,486	184
4	PA	509,096	286
5	KY	362,342	112
6	IL	340,054	232
7	MI	284,742	175
8	MO	271,120	88
9	AL	224,286	96
10	WV	185,756	77
		⋮	
17	GA	127,018	176

Solar photo voltaic generation continues to decrease in cost, and expand in application via solar roofing. Solar power can also provide reduced dependence on fossil fuel power plants. Because of the temporal nature of solar power, the APOM approach could be used to more accurately value the contribution of solar power to reductions in human health impacts.

Outside of power generation, air pollutant impacts from transportation is another promising area of investigation. Potential coordinated decisions using dynamic toll pricing could be applied to reduce health impacts on poor air quality days. Pricing could be optimized via mathematical models that trade off increased tolls with decreased air pollution. Additionally, highway design or redesign could be evaluated using an air quality modeling framework.

5.1.3 APOM refinements and improvements

APOM is a new approach that can be strengthened through validation and assessment of its uncertainties and limitations. Areas for investigation could include improved quantification of air pollutant sensitivities, improved pollutant health impact estimation, improved decisions using stochastic optimization that account for demand and air quality uncertainty, and improved optimization decisions via inclusion of transmission costs within APOM.

Refining air pollutant emissions sensitivities is possible in several ways. One difficulty is not being able to quantify the uncertainty in air pollutant formation from changes in a point source emitter. Estimating uncertainties could be possible in part by using second-order and other higher-order terms of the Taylor series expansion. Alternatively re-simulating under randomly perturbed initial conditions may yield a range of values for pollutant formation from a point-source emitter. These uncertainties could then be used to estimate how decisions would change under a range of potential pollutant formation outcomes.

Agent-based simulation models could also improve health impact estimation. By integrating the time spent inside versus outside, and time spent near home versus near work could improve the exposure estimation from each individual in a sample set. These models could improve estimates of pollutant exposure experienced, and allow re-estimation of the connection between $PM_{2.5}$ exposure and increased mortality. Additionally they could improve the health impact estimates within APOM. Implementation of agent based models for health impact estimation would require detailed matching and calibration with the statistical studies that form the basis of health impact models.

Alternative methods for evaluating the connection between $PM_{2.5}$ exposure and increased mortality could also be possible by using an air quality simulation. Previous research uses the nearest air quality monitor in health-impact studies such as [28], [22]. The alternative method of using an air quality model could lead to validation or improved estimates of these correlations with mortality through leveraging the fine-spatial resolution of CMAQ instead of sparsely placed air quality stations.

Within APOM, stochastic optimization could improve unit commitment decisions under uncertainty. The computational burden could be managed by reducing the time scale to one or two poor air quality days, and focusing on two or three plants or demand-side management with substitutable generation (e.g., a coal plant, a natural gas plant, and a demand-side management plan). Focusing on two or three plants and a shorter time scale rather than a state-scale all-inclusive model as presented in this thesis could make such a model tractable.

Including transmission costs and constraints could improve the cost estimation within APOM. Although two plants may be able to substitute generation and reduce health impacts, transmission may make such decisions expensive or infeasible. Inclusion of these transmission variables in future iterations of APOM could clarify the conditions under which transmission limits APOM's application.

5.1.4 Conclusion

The interdisciplinary collaboration between atmospheric chemistry and operations research has a high potential that this thesis only begins to explore. From atmospheric simulation model creation and validation, to integrating health impacts and optimizing the production of energy or other goods, there are several paths of research in which the two areas can collaborate. The author suggests that these connections continue into the future and leverage the skills of each for both theoretical and applied research.

APPENDIX A

FIRST APPENDIX

Throughout Chapter II and Chapter III several input datasets are used. These are outlined in detail within the following section.

A.1 Model input data

Table 19: Abbreviations of fuel types and sub-types

Fuel Type	**Abbreviation**
Bituminous Coal	BIT
Sub-bituminous Coal	SUB
Natural Gas	NG
Water (Hydro)	WAT
Nuclear	NUC
Wood & Waste Biomass	WDS
Landfill Gas Biomass	LFG
Muni. Solid Biomass	MSB
Black Liquor Biomass	BLQ
Petroleum Coke	PC
Distillate Fuel Oil	DFO
Residual Fuel Oil	RFO

Table 20: Fuel Cost, Nominal $ / mmBtu

	Year							
Fuel Type	**2004**	**2005**	**2006**	**2007**	**2008**	**2009**	**2010**	**2011**
BIT	1.79	2.17	2.40	2.61	3.04	3.61	3.91	3.75
SUB	1.12	1.19	1.31	1.45	1.62	1.64	1.73	1.91
NG	6.38	10.17	7.08	7.25	10.05	4.54	5.09	4.64
WAT	0.00	0.00	0.00	0.00	0.00	0.00	0.00	0.00
NUC	0.43	0.44	0.44	0.49	0.46	0.52	0.63	0.75
WDS	1.46	2.28	2.32	2.42	2.66	2.20	2.40	2.43
LFG	1.46	2.28	2.32	2.42	2.66	2.20	2.40	2.43
MSB	1.46	2.28	2.32	2.42	2.66	2.20	2.40	2.43
BLQ	1.46	2.28	2.32	2.42	2.66	2.20	2.40	2.43
PC	0.94	1.40	1.55	1.92	2.41	2.48	3.06	3.82
DFO	8.77	12.52	14.10	15.82	16.22	12.46	17.04	22.85
RFO	4.49	7.49	10.30	8.90	13.42	9.39	12.87	19.14

Sources: EIA SEDS Data for Georgia Electricity Plant Generation Costs,
http://www.eia.gov/state/seds/data.cfm?incfile=/state/seds/sep_prices/eu/pr_eu_GA.html&sid=GA
Sub-bituminous coal price source (US annual average):
http://www.eia.gov/electricity/annual/html/epa_07_04.html

Biomass subtypes assumed to be EIA SEDS Georgia Wood & Waste Cost

Table 21: Heat Rate by Fuel Type, Btu / kWh

	Year							
Fuel Type	**2004**	**2005**	**2006**	**2007**	**2008**	**2009**	**2010**	**2011**
BIT	10,331	10,373	10,351	10,375	10,378	10,414	10,415	10,444
SUB	10,331	10,373	10,351	10,375	10,378	10,414	10,415	10,444
NG	8,647	8,551	8,471	8,403	8,305	8,159	8,185	8,152
WAT	0	0	0	0	0	0	0	0
NUC	10,428	10,436	10,435	10,489	10,452	10,459	10,452	10,464
WDS	6,651	6,651	6,651	6,651	6,651	6,651	6,651	6,651
LFG	12,838	12,838	12,838	12,838	12,838	12,838	12,838	12,838
MSB	13,500	13,500	13,500	13,500	13,500	13,500	13,500	13,500
BLQ	6,645	6,645	6,645	6,645	6,645	6,645	6,645	6,645
PC	10,571	10,631	10,809	10,794	11,015	10,923	10,984	10,829
DFO	10,571	10,631	10,809	10,794	11,015	10,923	10,984	10,829
RFO	10,571	10,631	10,809	10,794	11,015	10,923	10,984	10,829

Sources: Coal, Gas, Nuclear, Petroleum from EIA Electric Power Annual national averages, http://www.eia.gov/electricity/annual/html/epa_08_01.html
Biomass plants taken from EPA eGRID 2004, 2006, 2007, and 2009 Georgia plants average across years, by sub-type (WDS, LFG, or BLQ)
Biomass MSB taken from EIA AEO 2012 heat rate estimate, 13,500 Btu/kWh.
Note that both WDS (wood and waste biomass) and BLQ (black liquor biomass) have lower than expected heat rates in EPA eGRID, possibly due to allocation of the heat from the combustion for process heat from the industrial facility.

Table 22: Nominal Fuel Cost by Fuel Type, $ / MWh

	Year							
Fuel Type	**2004**	**2005**	**2006**	**2007**	**2008**	**2009**	**2010**	**2011**
BIT	18.5	22.5	24.8	27.1	31.6	37.6	40.7	39.2
SUB	11.6	12.3	13.6	15.0	16.8	17.1	18.0	20.0
NG	55.2	87.0	60.0	60.9	83.5	37.0	41.7	37.8
WAT	0.0	0.0	0.0	0.0	0.0	0.0	0.0	0.0
NUC	4.5	4.6	4.6	5.1	4.8	5.4	6.6	7.9
WDS	9.7	15.2	15.4	16.1	17.7	14.6	16.0	16.2
LFG	18.7	29.3	29.8	31.1	34.2	28.2	30.8	31.2
MSB	19.7	30.8	31.3	32.7	35.9	29.7	32.4	32.8
BLQ	9.7	15.2	15.4	16.1	17.7	14.6	16.0	16.2
PC	9.9	14.9	16.8	20.7	26.6	27.1	33.6	41.4
DFO	92.7	133.1	152.4	170.8	178.7	136.1	187.2	247.4
RFO	47.5	79.6	111.3	96.1	147.8	102.6	141.4	207.3

Calculated: ($ / mmBtu) X (Btu / kWh) X (1 mmBtu / 1,000,000 Btu) X (1,000 kWh / MWh)

Table 23: US Consumer Price Index (CPI), used to adjust nominal costs to real costs, by year (CPI for 1982-84 = 100)

Year	CPI
2002	179.9
2003	184
2004	188.9
2005	195.3
2006	201.6
2007	207.34
2008	215.3
2009	214.54
2010	218.06
2011	224.94

Source: http://www.bls.gov/cpi/cpid1401.pdf, CPI Detailed Report Data for January 2014, Table 24, Historical Consumer Price Index for All Urban Consumers (CPI-U): U. S. city average, all items, Annual Average

Table 24: Real USD_{2007} Fuel Costs, \$ / MWh, by Fuel Type

	Year							
Fuel Type	**2004**	**2005**	**2006**	**2007**	**2008**	**2009**	**2010**	**2011**
BIT	20.3	23.9	25.6	27.1	30.4	36.3	38.7	36.1
SUB	12.7	13.1	14.0	15.0	16.2	16.5	17.1	18.4
NG	60.6	92.3	61.7	60.9	80.4	35.8	39.6	34.9
WAT	0.0	0.0	0.0	0.0	0.0	0.0	0.0	0.0
NUC	4.9	4.9	4.7	5.1	4.6	5.3	6.3	7.2
WDS	10.7	16.1	15.9	16.1	17.0	14.1	15.2	14.9
LFG	20.6	31.1	30.6	31.1	32.9	27.3	29.3	28.8
MSB	21.6	32.7	32.2	32.7	34.6	28.7	30.8	30.2
BLQ	10.7	16.1	15.9	16.1	17.0	14.1	15.2	14.9
PC	10.9	15.8	17.2	20.7	25.6	26.2	32.0	38.1
DFO	101.8	141.3	156.8	170.8	172.1	131.5	178.0	228.1
RFO	52.1	84.5	114.5	96.1	142.4	99.1	134.4	191.1

Source: Calculated, \$ / MWh [(Nominal Year \$ / MWh) X (CPI2007 / CPI Nominal Year)]

Table 25: Nominal Variable Operation Cost, $ / MWh

	Operation ($ / MWh)			
Year	**Nuclear**	**Fossil Steam**	**Hydro**	**Gas Turbine and Small Scale**
2004	8.97	3.13	3.83	4.27
2005	8.26	3.21	3.95	3.69
2006	9.03	3.57	3.76	3.51
2007	9.54	3.63	5.44	3.26
2008	9.89	3.72	5.78	3.77
2009	10	4.23	4.88	3.05
2010	10.5	4.04	5.33	2.79
2011	10.89	4.02	5.13	2.81

Source: http://www.eia.gov/electricity/annual/html/epa_08_04.html

Table 26: Nominal Variable Maintenance Cost, $ / MWh

	Maintenance ($ / MWh)			
Year	**Nuclear**	**Fossil Steam**	**Hydro**	**Gas Turbine and Small Scale**
2004	5.38	2.96	2.76	2.14
2005	5.27	2.98	2.73	1.89
2006	5.69	3.19	2.7	2.16
2007	5.79	3.37	3.87	2.42
2008	6.2	3.59	3.89	2.72
2009	6.34	3.96	3.5	2.58
2010	6.8	3.99	3.81	2.73
2011	6.8	3.99	3.74	2.93

Source: http://www.eia.gov/electricity/annual/html/epa_08_04.html

Table 27: Real USD_{2007} Variable O&M Cost, $ / MWh

Fuel Type	Nuclear	Fossil Steam	Hydro	Gas Turbine and Small Scale
2004	15.75	6.68	7.23	7.04
2005	14.36	6.57	7.09	5.92
2006	15.14	6.95	6.64	5.83
2007	15.33	7	9.31	5.68
2008	15.5	7.04	9.31	6.25
2009	15.79	7.92	8.1	5.44
2010	16.45	7.64	8.69	5.25
2011	16.31	7.38	8.18	5.29

Source: Calculated, CPI adjusted to USD2007 Coal assumed to be Fossil Steam. Natural Gas, Biomass sub-types and Petroleum sub-types assumed to be Gas Turbine and Small Scale.

Table 28: Variable Fuel and O&M Cost, by Fuel Type, $ / MWh, Real USD_{2007}

	Year							
	2004	**2005**	**2006**	**2007**	**2008**	**2009**	**2010**	**2011**
BIT	$26.98	$30.47	$32.50	$34.08	$37.42	$44.25	$46.36	$43.48
SUB	$19.38	$19.68	$20.90	$22.04	$23.23	$24.42	$24.77	$25.77
NG	$67.59	$98.25	$67.51	$66.60	$86.63	$41.24	$44.86	$40.16
WAT	$7.23	$7.09	$6.64	$9.31	$9.31	$8.10	$8.69	$8.18
NUC	$20.67	$19.24	$19.86	$20.47	$20.13	$21.05	$22.71	$23.54
WDS	$17.69	$22.02	$21.70	$21.77	$23.29	$19.58	$20.43	$20.19
LFG	$27.61	$37.00	$36.46	$36.75	$39.14	$32.74	$34.55	$34.05
MSB	$28.67	$38.60	$38.04	$38.35	$40.83	$34.15	$36.06	$35.53
BLQ	$17.68	$22.01	$21.69	$21.76	$23.27	$19.57	$20.41	$20.18
PC	$17.94	$21.73	$23.06	$26.40	$31.81	$31.62	$37.21	$43.42
DFO	$108.79	$147.23	$162.58	$176.44	$178.31	$136.98	$183.22	$233.38
RFO	$59.13	$90.46	$120.34	$101.75	$148.61	$104.57	$139.67	$196.34

Source: Calculated, Variable Fuel Cost + Variable O&M Cost

Table 29: Average annual SO_2 emissions rates (lbs / MWh) by fuel subtype for US electricity generating plants

	Year							
Fuel Type	**2004**	**2005**	**2006**	**2007**	**2008**	**2009**	**2010**	**2011**
BIT	12.119	11.793	11.793	10.732	10.732	7.272	5.562	5.562
SUB	6.234	6.377	6.377	6.159	6.159	5.490	5.364	5.364
NG	0.151	0.109	0.109	0.136	0.136	0.126	0.118	0.118
WAT	0.000	0.000	0.000	0.000	0.000	0.000	0.000	0.000
NUC	0.000	0.000	0.000	0.000	0.000	0.000	0.000	0.000
WDS	0.920	1.513	1.513	1.668	1.668	1.549	1.665	1.665
LFG	0.002	0.000	0.000	0.003	0.003	0.002	0.002	0.002
MSB	(no data)	0.611	0.611	39.150*	39.150*	7.982	8.220	8.220
BLQ	4.932	4.096	4.096	3.787	3.787	3.283	3.640	3.640
PC	5.880	12.392	12.392	16.209	16.209	8.640	8.136	8.136
DFO	0.362	0.530	0.530	0.261	0.261	0.191	0.144	0.144
RFO	6.987	6.880	6.880	7.273	7.273	6.975	3.861	3.861

Source: All plants in the US from EPA eGRID for the available years: 2004, 2005, 2007, 2009, 2010. Emissions rates are averaged for plants in the US by fuel type, by summing total SO_2 emissions (lbs), and dividing by annual net generation (MWh), equivalent to a net generation weighted average. For years without data, the previous year estimate is used. For example, year 2006 emissions are not available via eGRID, so the year 2005 value was used.

* Municipal solid biomass (MSB) has highly varied values during the first years that eGRID included MSB within eGRID (years 2005 and 2007).

Table 30: Average annual SO_2 emissions rates (lbs / MWh) by fuel subtype for GA electricity generating plants

	Year							
Fuel Type	**2004**	**2005**	**2006**	**2007**	**2008**	**2009**	**2010**	**2011**
BIT	16.555	16.894	16.894	17.158	17.158	8.332	5.992	5.992
SUB	6.856	6.881	6.881	6.103	6.103	6.051	6.049	6.049
NG	0.016	0.007	0.007	0.005	0.005	0.012	0.006	0.006
WAT	0.000	0.000	0.000	0.000	0.000	0.000	0.000	0.000
NUC	0.000	0.000	0.000	0.000	0.000	0.000	0.000	0.000
WDS	0.223	4.112	4.112	0.243	0.243	4.147	4.033	4.033
LFG	0.000	0.000	0.000	0.000	0.000	0.000	0.000	0.000
MSB*	23.410	23.410	23.410	33.793	33.793	33.793	33.793	33.793
BLQ	3.490	4.561	4.561	3.782	3.782	3.022	3.066	3.066
PC*	51.816	51.816	51.816	37.611	37.611	28.132	34.620	34.620
DFO	4.444	2.700	2.700	1.780	1.780	25.673	27.187	27.187
RFO*	22.788	31.613	31.613	38.391	38.391	38.391	38.391	38.391

Source: Georgia plants only from EPA eGRID for the available years: 2004, 2005, 2007, 2009, 2010. Emissions rates are averaged for all plants in the US, by fuel type, by summing total SO_2 emissions (lbs), and dividing by annual net generation (MWh), equivalent to a net generation weighted average. For years without available data, the previous years estimate is used. For example, year 2006 emissions are not available via eGRID, so the year 2005 value was used.

* MSB, PC and RFO have limited data, so previous year data is used when data is not available (years 2005-2006 and 2008-2011 for MSB; years 2008-2011 for RFO; and years 2005-2006 for PC).

Table 31: Average January SO_2 emissions rates (lbs / MWh) from coal generation point sources

	Year							
Plant	**2004**	**2005**	**2006**	**2007**	**2008**	**2009**	**2010**	**2011**
Bowen	15.35	15.99	17.48	15.28	11.89	3.55	0.6	0.41
Hammond	18.71	16.4	17.94	17.03	0.31	0.37	1.49	1.51
Harllee	17.86	18.99	17.86	18.06	16.57	16.97	17.89	19.28
McDonough	13.25	13.56	14.41	13.98	14.54	13.81	14.8	16.24
Scherer	6.42	6	5.89	5.76	6.3	5.83	6.12	4.61
Wansley	13.22	12.98	11.64	10.86	10.46	0.2	0.32	0.55
Yates	16.72	16.96	20.81	20.61	15.23	17.72	16.1	18.89

Source: EPA Continuous Emissions Monitoring Data (ftp://ftp.epa.gov), Averaged for January 2004 through 2011, accessed June 16, 2014.

Table 32: Average July SO_2 emissions rates (lbs / MWh) from coal fueled point sources

	Year							
Plant	**2004**	**2005**	**2006**	**2007**	**2008**	**2009**	**2010**	**2011**
Bowen	16.01	14.14	17.47	16.55	16.58	8.6	1.54	0.72
Hammond	18.82	13.7	19.42	19.85	17.75	0.11	0.6	0.74
Harllee	15.83	17.86	16.38	17.36	18.79	16.59	15.44	19.23
McDonough	12.22	12.22*	14.53	13.22	14.36	14.31	14.31*	14.87
Scherer	6.71	6.24	6.28	5.77	5.58	5.8	5.56	5.17
Wansley	14.76	12.99	15.03	13.87	9.74	9.33	0.2	0.41
Yates	15.71	21.36	16.96	18.64	19.28	16.36	19.63	18.49

Source: EPA Continuous Emissions Monitoring Data (ftp://ftp.epa.gov), Averaged for July 2004 through 2011, accessed June 16, 2014.
Plant Scherer uses lower sulfur content subbituminous coal, while the remaining coal plants use bituminous coal.

* Plant McDonough previous year data is used for 2005 and 2010 due to lack of data available in July of those years.

Table 33: Value of Statistical Life (VSL) Estimates, EPA 2010, Real USD_{2007}

Author(s) (Year)	USD2007 VSL (millions)
Kniesner and Leeth (1991 - US)^L	0.87
Smith and Gilbert (1984)^L	0.99
Dillingham (1985)^L	1.37
Butler (1983)^L	1.62
Miller and Guria (1991)^C	1.87
Moore and Viscusi (1988)^L	3.73
Viscusi, Magat, and Huber (1991)^C	4.11
Marin and Psacharopoulos (1982)^L	4.23
Gegax et al. (1985)^C	4.98
Kniesner and Leeth (1991 - Australia)^L	4.98
Gerking, de Haan, and Schulze (1988)^C	5.1
Cousineau, Lecroix, and Girard (1988)^L	5.47
Jones-Lee (1989)^C	5.73
Dillingham (1985)^L	5.85
Viscusi (1978)^L	6.22
R.S. Smith (1976)^L	6.97
V.K. Smith (1983)^L	7.09
Olson (1981)^L	7.84
Viscusi (1981)^L	9.84
R.S. Smith (1974)^L	10.83
Moore and Viscusi (1988)^L	10.96
Kniesner and Leeth (1991 - Japan)^L	11.46
Herzog and Schlottman (1987)^L	13.69
Leigh and Folsom (1984)^L	14.56
Leigh (1987)^L	15.69
Garen (1988)^L	20.29

Source: Guidelines for Preparing Economic Analyses: Mortality Risk Valuation Estimates, Report Number: EE-0568. Retrieved July 27, 2015 from http://yosemite.epa.gov/ee/epa/eerm.nsf/vwAN/EE-0568-22.pdf.
^{L} indicates a labor market estimate
^{C} indicates a contingent valuation estimate

Table 34: Power Plants Greater than 500 MW in Nameplate Capacity

Plant Name	Type (Subtype)	Capacity in MW (Capacity Factor)	Group Source	ORIS
Bowen	Coal (BIT)	3540.4 (0.8)		703
Wansley	Coal (BIT)	1956.8 (0.8)	North Georgia	6052
Harllee Branch	Coal (BIT)	1746.2 (0.8)	North Georgia	709
Yates	Coal (BIT)	1487.3 (0.8)		728
McIntosh	Coal (BIT)	988 (0.8)	South Georgia	6124
Hammond	Coal (BIT)	953 (0.8)	North Georgia	708
Jack McDonough	Coal (BIT)	682 (0.8)		710
Scherer	Coal (SUB)	3564 (0.8)		6257
McIntosh Combined Cycle	Gas (NG)	1376.6 (0.8)	South Georgia	56150
Wansley Combined Cycle	Gas (NG)	1239 (0.8)		55965
KGen Murray I and II LLC	Gas (NG)	1192 (0.8)	North Georgia	55382
Tenaska GA Generation	Gas (NG)	1099.2 (0.8)	North Georgia	55061
Dahlberg	Gas (NG)	919 (0.8)	North Georgia	7709
Washington County	Gas (NG)	797.6 (0.8)	North Georgia	55332
Talbot County Energy	Gas (NG)	726 (0.8)	South Georgia	7916
West Georgia Generating	Gas (NG)	701.2 (0.8)	South Georgia	55267
Sandersville	Gas (NG)	692 (0.8)	North Georgia	55672
Walton County Power LLC	Gas (NG)	612 (0.8)	North Georgia	55128
Effingham County Power Project	Gas (NG)	594.3 (0.8)	South Georgia	55406
Sewell Creek Energy	Gas (NG)	570 (0.8)	North Georgia	7813
Wansley Unit 9	Gas (NG)	568 (0.8)		7946
Chattahoochee Energy	Gas (NG)	539.7 (0.8)		7917
Richard B Russell	Hydro (WAT)	628 (0.09)		6132
Carters	Hydro (WAT)	500 (0.12)		6130
Vogtle	Nuclear (NUC)	2320 (0.95)		649
Edwin I Hatch	Nuclear (NUC)	1721.8 (0.95)		6051
McManus	Oil (RFO)	644.3 (0.5)	South Georgia	715

Table 35: Power Plants Less Than 500 MW and Greater Than 72 MW in Nameplate Capacity

Plant Name	Type (Subtype)	Capacity in MW (Capacity Factor)	Group Source	ORIS
International Paper Savanna Mill	Biomass (BLQ)	154 (0.8)	South Georgia	50398
Georgia Pacific Cedar Springs	Biomass (BLQ)	101.2 (0.8)	South Georgia	54101
International Paper Augusta Mill	Biomass (BLQ)	84.7 (0.8)	North Georgia	54358
Rayonier Jesup Mill	Biomass (BLQ)	82 (0.8)	South Georgia	10560
Port Wentworth Mill	Biomass (BLQ)	72.3 (0.8)	South Georgia	50804
Brunswick Cellulose	Biomass (BLQ)	72.2 (0.8)	South Georgia	10605
Kraft	Coal (BIT)	352.4 (0.8)	South Georgia	733
Mitchell	Coal (BIT)	288.6 (0.8)	South Georgia	727
Dublin Mill	Coal (BIT)	82.1 (0.8)	South Georgia	54004
Heard County Power LLC	Gas (NG)	495 (0.8)	North Georgia	55141
Doyle Generating Facility	Gas (NG)	409 (0.8)	North Georgia	55244
MPC Generating	Gas (NG)	386.1 (0.8)	North Georgia	7764
Hartwell Energy LP	Gas (NG)	360 (0.8)	North Georgia	54538
Mid-Georgia Cogeneration Facility	Gas (NG)	323 (0.8)	South Georgia	55040
Smarr Energy Center	Gas (NG)	242 (0.8)	South Georgia	7829
Baconton Power Plant	Gas (NG)	240 (0.8)	South Georgia	55304
Robins	Gas (NG)	183.8 (0.8)	South Georgia	7348
Sowega Power	Gas (NG)	120 (0.8)	South Georgia	7768
Hartwell Lake	Hydro (WAT)	420 (0.068)		754
Buford	Hydro (WAT)	131.2 (0.105)		759
Walter F George	Hydro (WAT)	130 (0.183)		761
Allatoona	Hydro (WAT)	86.6 (0.067)		760
West Point	Hydro (WAT)	73.3 (0.141)		6133
Tallulah Falls	Hydro (WAT)	72 (0.096)		723
Wilson	Oil (DFO)	321.2 (0.5)	North Georgia	6258
Bainbridge	Oil (DFO)	80 (0.5)	South Georgia	56015
Savannah River Mill	Oil (PC)	140.4 (0.5)	South Georgia	10361

Table 36: Power Plants Less Than 72 MW and Greater Than four MW in Nameplate Capacity

Plant Name	Type	Capacity in MW (Capacity Factor)	Group Source	ORIS
Inland Paperboard Packaging Rome	Biomass (BLQ)	70.4 (0.8)	North Georgia	10426
Flint River Operations	Biomass (BLQ)	42 (0.8)	South Georgia	50465
Riverwood International Macon Mill	Biomass (BLQ)	33.4 (0.8)	South Georgia	54464
Brunswick Plant	Biomass (WDS)	9.1 (0.8)	South Georgia	10605
Crisp Plant	Coal (BIT)	17.5 (0.8)	South Georgia	753
Savannah Sugar Refinery	Coal (BIT)	11.7 (0.8)	South Georgia	50146
Kamin LLC Wrens Plant	Gas (NG)	10.4 (0.5)	North Georgia	54880
Oliver Dam	Hydro (WAT)	60 (0.208)		720
Sinclair Dam	Hydro (WAT)	45 (0.106)		722
Tugalo	Hydro (WAT)	44.8 (0.129)		725
North Highlands	Hydro (WAT)	29.6 (0.259)		719
Blue Ridge	Hydro (WAT)	23.5 (0.078)		757
Yonah	Hydro (WAT)	22.5 (0.109)		729
Stevens Creek	Hydro (WAT)	18.4 (0.362)		736
Lake Blackshear Project	Hydro (WAT)	17.2 (0.183)		752
Morgan Falls	Hydro (WAT)	16.8 (0.185)		717
Terrora	Hydro (WAT)	16 (0.147)		724
Nottely	Hydro (WAT)	15.9 (0.087)		758
Lloyd Shoals	Hydro (WAT)	14.4 (0.275)		712
Burton	Hydro (WAT)	6 (0.207)		704
Flint River	Hydro (WAT)	5.4 (0.471)		706
Nacoochee	Hydro (WAT)	4.8 (0.153)		718
Eagle & Phenix	Hydro (WAT)	4.2 (0.068)		54470
Naval Submarine Base Kings Bay	Oil (DFO)	30 (0.5)	South Georgia	54239
State Farm Insurance Support Center East	Oil (DFO)	10.8 (0.5)	North Georgia	55274
YKK USA Chestney	Oil (DFO)	6.8 (0.5)	South Georgia	54566
Athens Regional Medical Center	Oil (DFO)	4.5 (0.5)	North Georgia	55319

Table 37: Power Plants Less Than four MW in Nameplate Capacity

Plant Name	Type	Capacity Factor (Model)	Group Source	ORIS
BJ Gas Recovery	Biomass (LFG)	2.4 (0.8)	North Georgia	54392
Riverside Manufacturing	Gas (NG)	1.1 (0.8)	South Georgia	54856
Barnett Shoals	Hydro (WAT)	2.8 (0.051)		701
Avondale Mills	Hydro (WAT)	2.1 (0.632)		54322
High Shoals Hydro	Hydro (WAT)	1.4 (0.004)		10121
Graniteville Enterprise Division	Hydro (WAT)	1.2 (0.481)		54462
Milstead	Hydro (WAT)	1 (0.136)		54872
Dekalb Medical Center	Oil (DFO)	3.9 (0.5)	North Georgia	54830
Valdosta Water Treatment Plant	Oil (DFO)	3.4 (0.5)	South Georgia	54839
Bank of America Plaza	Oil (DFO)	3 (0.5)	North Georgia	55152
Sun Trust Plaza	Oil (DFO)	2.4 (0.5)	North Georgia	54845
Thiele Kaolin Sandersville	Oil (DFO)	2.4 (0.5)	South Georgia	54841
Thiele Kaolin Reedy Creek	Oil (DFO)	2.2 (0.5)	North Georgia	54849
South Georgia Medical Center	Oil (DFO)	1.9 (0.5)	South Georgia	54848
Shepherd Center	Oil (DFO)	1.7 (0.5)	North Georgia	54813
DeKalb Medical Center-Hillandale	Oil (DFO)	1.6 (0.5)	North Georgia	56231
Riverwood 100 Building	Oil (DFO)	1.1 (0.5)	North Georgia	54816

Table 38: Population estimates by year via intercensal population estimates. Also expressed as a fraction of 2010 US Census population estimate.

Year	Georgia Population Estimate	% of 2010 Census Value
2004†	8,769,252	90.50%
2005†	8,925,922	92.10%
2006†	9,155,813	94.50%
2007†	9,349,988	96.50%
2008†	9,504,843	98.10%
2009†	9,620,846	99.30%
2010*†	9,687,653	100.00%
2011‡	9,812,460	101.30%

† **Source:** U.S. Census Bureau, Population Division, Table 1. Intercensal Estimates of the Resident Population for the United States, Regions, States, and Puerto Rico: April 1, 2000 to July 1, 2010 (ST-EST00INT-01), Release Date: September 2011
* **Source:** 2010 US Census count
‡ **Source:** U.S. Census Bureau, Population Division, Table 1. Annual Estimates of the Population for the United States, Regions, States, and Puerto Rico: April 1, 2010 to July 1, 2012 (NST-EST2012-01), Release Date: December 2012

Table 39: Power Plants Startup Cost Estimates

	Gas, Biomass, Oil	Coal
Startup cost ($ / MW, USD2011)	$72	$105

Source: Kumar N, Besuner P, Lefton S, Agan D, and Hilleman D (2012). Power Plant Cycling Costs. Intertek APTECH Subcontract Report. NREL/SR-5500-55433. Available at http://www.nrel.gov/docs/fy12osti/55433.pdf.

REFERENCES

[1] Benitez, L. E., Benitez, P. C., and van Kooten, G. C., "The economics of wind power with energy storage," *Energy Economics*, vol. 30, pp. 1973–1989, Jul 2008.

[2] Boylan, J. W., Odman, M. T., Wilkinson, J. G., and Russell, A. G., "Integrated assessment modeling of atmospheric pollutants in the Southern Appalachian Mountains: Part II. Fine particulate matter and visibility.," *Journal of the Air & Waste Management Association (1995)*, vol. 56, pp. 12–22, Jan 2006.

[3] Boylan, J. W. and Russell, A. G., "PM and light extinction model performance metrics, goals, and criteria for three-dimensional air quality models," *Atmospheric Environment*, vol. 40, pp. 4946–4959, Aug 2006.

[4] Byun, D. and Schere, K. L., "Review of the Governing Equations, Computational Algorithms, and Other Components of the Models-3 Community Multiscale Air Quality (CMAQ) Modeling System," *Applied Mechanics Reviews*, vol. 59, no. 2, p. 51, 2006.

[5] Caiazzo, F., Ashok, A., Waitz, I. A., Yim, S. H., and Barrett, S. R., "Air pollution and early deaths in the United States. Part I: Quantifying the impact of major sectors in 2005," *Atmospheric Environment*, vol. 79, pp. 198–208, Nov 2013.

[6] Centers for Disease Control and Prevention National Center for Health Statistics (CDC NCHS), "Underlying Cause of Death 1999-2010. CDC WONDER Online Database," 2015.

[7] Cohan, D. S., Hakami, A., Hu, Y., and Russell, A. G., "Nonlinear Response of Ozone to Emissions: Source Apportionment and Sensitivity Analysis," *Environmental Science & Technology*, vol. 39, pp. 6739–6748, Sep 2005.

[8] Cohan, D. S., Tian, D., Hu, Y., and Russell, A. G., "Control Strategy Optimization for Attainment and Exposure Mitigation: Case Study for Ozone in Macon, Georgia," *Environmental Management*, vol. 38, pp. 451–462, Sep 2006.

[9] Cropper, M., Gamkhar, S., Malik, K., Limonov, A., and Partridge, I., "Health Effects of Coal Electricity Generation in India," 2012.

[10] Daniels, M. J., Dominici, F., Samet, J. M., and Zeger, S. L., "Estimating particulate matter-mortality dose-response curves and threshold levels: an analysis of daily time-series for the 20 largest US cities.," *American journal of epidemiology*, vol. 152, pp. 397–406, Sep 2000.

[11] Guo, H., Xu, L., Bougiatioti, A., Cerully, K. M., Capps, S. L., Hite, J. R., Carlton, A. G., Lee, S.-H., Bergin, M. H., Ng, N. L., Nenes, A., and Weber, R. J., "Fine-particle water and pH in the southeastern United States," *Atmospheric Chemistry and Physics*, vol. 15, pp. 5211–5228, May 2015.

[12] Gurobi Optimization Incorporated, "Gurobi Optimizer Version 5.1.0," 2014.

[13] Hakami, A., Odman, M. T., and Russell, A. G., "High-Order, Direct Sensitivity Analysis of Multidimensional Air Quality Models," *Environmental Science & Technology*, vol. 37, pp. 2442–2452, jun 2003.

[14] Hedman, K. W., O'Neill, R. P., and Oren, S. S., "Analyzing valid inequalities of the generation unit commitment problem," in *2009 IEEE/PES Power Systems Conference and Exposition*, pp. 1–6, IEEE, Mar 2009.

[15] Hobbs, B. F., Rothkopf, M. H., O'Neill, R. P., and Chao, H.-p., eds., *The Next Generation of Electric Power Unit Commitment Models*, vol. 36 of *International Series in Operations Research & Management Science*. Boston: Kluwer Academic Publishers, 2002.

[16] Hodan, W. M. and Barnard, W. R., "Evaluating the Contribution of PM2.5 Precursor Gases and Re-entrained Road Emissions to Mobile Source PM2.5 Particulate Matter Emissions," 2004.

[17] Hu, Y., Odman, M. T., Chang, M. E., and Russell, A. G., "Operational forecasting of source impacts for dynamic air quality management," *Atmospheric Environment*, vol. 116, pp. 320–322, Sep 2015.

[18] Kerl, P. Y., Zhang, W., Moreno-Cruz, J. B., Nenes, A., Realff, M. J., Russell, A. G., Sokol, J., and Thomas, V. M., "New approach for optimal electricity planning and dispatching with hourly time-scale air quality and health considerations," *Proceedings of the National Academy of Sciences*, vol. 112, pp. 10884–10889, sep 2015.

[19] Kim, B.-U., Kim, O., Kim, H. C., and Kim, S., "Influence of fossil-fuel power plant emissions on the surface fine particulate matter in the Seoul Capital Area, South Korea," *Journal of the Air & Waste Management Association*, vol. 66, pp. 863–873, sep 2016.

[20] Kirby, B. and Hirst, E., "Generator response to intrahour load fluctuations," *IEEE Transactions on Power Systems*, vol. 13, no. 4, pp. 1373–1378, 1998.

[21] Kochi, I., Hubbell, B. J., and Kramer, R., "An empirical Bayes approach to combining and comparing estimates of the value of a statistical life for environmental policy analysis," *Environmental and Resource Economics*, vol. 34, pp. 385–406, Jul 2006.

[22] Krewski, D., Jerrett, M., Burnett, R. T., Ma, R., Hughes, E., Shi, Y., Turner, M. C., Pope, C. A., Thurston, G., Calle, E. E., Thun, M. J., Beckerman, B., DeLuca, P., Finkelstein, N., Ito, K., Moore, D. K., Newbold, K. B., Ramsay, T., Ross, Z., Shin, H., and Tempalski, B., "Extended follow-up and spatial analysis of the American Cancer Society study linking particulate air pollution and mortality.," *Research report (Health Effects Institute)*, pp. 5–114; discussion 115–36, May 2009.

[23] Lim, S. S., Vos, T., Flaxman, A. D., Danaei, G., Shibuya, K., Adair-Rohani, H., AlMazroa, M. A., Amann, M., Anderson, H. R., Andrews, K. G., Aryee, M., Atkinson, C., Bacchus, L. J., Bahalim, A. N., Balakrishnan, K., Balmes, J., Barker-Collo, S., Baxter, A., Bell, M. L., Blore, J. D., Blyth, F., Bonner, C., Borges, G., Bourne, R., Boussinesq, M., Brauer, M., Brooks, P., Bruce, N. G., Brunekreef, B., Bryan-Hancock, C., Bucello, C., Buchbinder, R., Bull, F., Burnett, R. T., Byers, T. E., Calabria, B., Carapetis, J., Carnahan, E., Chafe, Z., Charlson, F., Chen, H., Chen, J. S., Cheng, A. T.-A., Child, J. C., Cohen, A., Colson, K. E., Cowie, B. C., Darby, S., Darling, S., Davis, A., Degenhardt, L., Dentener, F., Des Jarlais, D. C., Devries, K., Dherani, M., Ding, E. L., Dorsey, E. R., Driscoll, T., Edmond, K., Ali, S. E., Engell, R. E., Erwin, P. J., Fahimi, S., Falder, G., Farzadfar, F., Ferrari, A., Finucane, M. M., Flaxman, S., Fowkes, F. G. R., Freedman, G., Freeman, M. K., Gakidou, E., Ghosh, S., Giovannucci, E., Gmel, G., Graham, K., Grainger, R., Grant, B., Gunnell, D., Gutierrez, H. R., Hall, W., Hoek, H. W., Hogan, A., Hosgood, H. D., Hoy, D., Hu, H., Hubbell, B. J., Hutchings, S. J., Ibeanusi, S. E., Jacklyn, G. L., Jasrasaria, R., Jonas, J. B., Kan, H., Kanis, J. A., Kassebaum, N., Kawakami, N., Khang, Y.-H., Khatibzadeh, S., Khoo, J.-P., Kok, C., Laden, F., Lalloo, R., Lan, Q., Lathlean, T., Leasher, J. L., Leigh, J., Li, Y., Lin, J. K., Lipshultz, S. E., London, S., Lozano, R., Lu, Y., Mak, J., Malekzadeh, R., Mallinger, L., Marcenes, W., March, L., Marks, R., Martin, R., McGale, P., McGrath, J., Mehta, S., Memish, Z. A., Mensah, G. A., Merriman, T. R., Micha, R., Michaud, C., Mishra, V., Hanafiah, K. M., Mokdad, A. A., Morawska, L., Mozaffarian, D., Murphy, T., Naghavi, M., Neal, B., Nelson, P. K., Nolla, J. M., Norman, R., Olives, C., Omer, S. B., Orchard, J., Osborne, R., Ostro, B., Page, A., Pandey, K. D., Parry, C. D., Passmore, E., Patra, J., Pearce, N., Pelizzari, P. M., Petzold, M., Phillips, M. R., Pope, D., Pope, C. A., Powles, J., Rao, M., Razavi, H., Rehfuess, E. A., Rehm, J. T., Ritz, B., Rivara, F. P., Roberts, T., Robinson, C., Rodriguez-Portales, J. A., Romieu, I., Room, R., Rosenfeld, L. C., Roy, A., Rushton, L., Salomon, J. A., Sampson, U., Sanchez-Riera, L., Sanman, E., Sapkota, A., Seedat, S., Shi, P., Shield, K., Shivakoti, R., Singh, G. M., Sleet, D. A., Smith, E., Smith, K. R., Stapelberg, N. J., Steenland,

K., Stöckl, H., Stovner, L. J., Straif, K., Straney, L., Thurston, G. D., Tran, J. H., Van Dingenen, R., van Donkelaar, A., Veerman, J. L., Vijayakumar, L., Weintraub, R., Weissman, M. M., White, R. A., Whiteford, H., Wiersma, S. T., Wilkinson, J. D., Williams, H. C., Williams, W., Wilson, N., Woolf, A. D., Yip, P., Zielinski, J. M., Lopez, A. D., Murray, C. J., and Ezzati, M., "A comparative risk assessment of burden of disease and injury attributable to 67 risk factors and risk factor clusters in 21 regions, 19902010: a systematic analysis for the Global Burden of Disease Study 2010," *The Lancet*, vol. 380, pp. 2224–2260, Dec 2012.

[24] Muller, N. Z. and Mendelsohn, R., "The Air Pollution Emission Experiments and Policy Analysis Model (APEEP)," 2006.

[25] Muller, N. Z., Mendelsohn, R., and Nordhaus, W., "Environmental Accounting for Pollution in the United States Economy," *American Economic Review*, vol. 101, pp. 1649–1675, Aug 2011.

[26] Napelenok, S. L., Cohan, D. S., Hu, Y., and Russell, A. G., "Decoupled direct 3D sensitivity analysis for particulate matter (DDM-3D/PM)," *Atmospheric Environment*, vol. 40, pp. 6112–6121, Oct 2006.

[27] Nemhauser, G. and Wolsey, L., *Integer and Combinatorial Optimization*. Hoboken, NJ, USA: John Wiley & Sons, Inc., Jun 1988.

[28] Pope III, C. A., "Lung Cancer, Cardiopulmonary Mortality, and Long-term Exposure to Fine Particulate Air Pollution," *JAMA*, vol. 287, p. 1132, Mar 2002.

[29] Siler-Evans, K., Azevedo, I. L., Morgan, M. G., and Apt, J., "Regional variations in the health, environmental, and climate benefits of wind and solar generation," *Proceedings of the National Academy of Sciences*, vol. 110, pp. 11768–11773, Jul 2013.

[30] Simon, H., Baker, K. R., Akhtar, F., Napelenok, S. L., Possiel, N., Wells, B., and Timin, B., "A Direct Sensitivity Approach to Predict Hourly Ozone Resulting from Compliance with the National Ambient Air Quality Standard," *Environmental Science & Technology*, vol. 47, pp. 2304–2313, Mar 2013.

[31] US Census, "Annual Estimates of the Resident Population for the United States, Regions, States, and Puerto Rico: April 1, 2010 to July 1, 2015," 2015.

[32] U.S. Department of Commerce - Economics and Statistics Administration - Bureau of the Census, *Geographic areas reference manual*. Washington, D.C.: US Bureau of the Census, 1994.

[33] US Energy Information Administration, "Annual Energy Outlook 2013," 2013.

[34] US Energy Information Administration, "Electric Power Annual 2013," 2013.

[35] U.S. Energy Information Administration, "June 2014 Monthly Energy Review," 2014.

[36] US Energy Information Administration, "Electric Power Detailed State Data," 2016.

[37] US Energy Information Administration State Energy Data System (EIA SEDS), "State Energy Data System (SEDS): 1960-2011 (Complete)," 2011.

[38] US Environmental Protection Agency, "EPA Emissions & Generation Resource Integrated Database (eGRID) Ninth Edition," 2011.

[39] US Environmental Protection Agency (EPA), "Guidelines for Preparing Economic Analyses: Mortality Risk Valuation Estimates," 2010.

[40] U.S. Environmental Protection Agency (EPA), "Acid Rain Program," 2012.

[41] U.S. Environmental Protection Agency (EPA), "National Ambient Air Quality Standards (NAAQS)," 2012.

[42] US Environmental Protection Agency (EPA), "US EPA BenMAP Manual Appendice," 2012.

[43] US Environmental Protection Agency (EPA), "US EPA BenMAP," 2013.

[44] U.S. Environmental Protection Agency (EPA), "Cross-State Air Pollution Rule (CSAPR)," 2014.

[45] US Environmental Protection Agency (EPA), "US Continuous Emissions Monitoring Data," 2014.

[46] US Environmental Protection Agency (EPA), "US Continuous Emissions Monitoring Factsheet," 2014.

[47] US Environmental Protection Agency (EPA), "Environmental Justice," 2016.

[48] Yang, Y.-J., Wilkinson, J. G., and Russell, A. G., "Fast, Direct Sensitivity Analysis of Multidimensional Photochemical Models," *Environmental Science & Technology*, vol. 31, pp. 2859–2868, Oct 1997.

[49] Zhang, W., Capps, S. L., Hu, Y., Nenes, A., Napelenok, S. L., and Russell, A. G., "Development of the high-order decoupled direct method in three dimensions for particulate matter: enabling advanced sensitivity analysis in air quality models," *Geoscientific Model Development*, vol. 5, pp. 355–368, Mar 2012.

[50] Zheng, M., Cass, G. R., Ke, L., Wang, F., Schauer, J. J., Edgerton, E. S., and Russell, A. G., "Source Apportionment of Daily Fine Particulate Matter at Jefferson Street, Atlanta, GA, during Summer and Winter," *Journal of the Air & Waste Management Association*, vol. 57, pp. 228–242, Feb 2007.